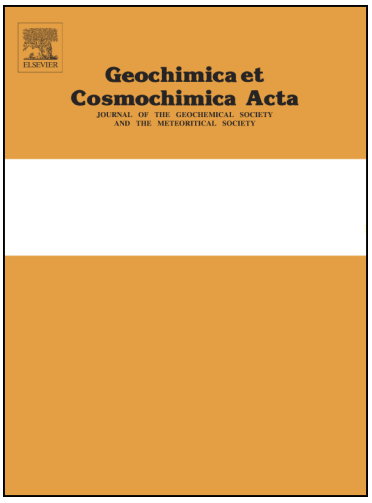

The stoichiometric dissociation constants of carbonic acid in seawater brines from 298 to 267 K

Stathys Papadimitriou, Socratis Loucaides, Victoire M.C. Rérolle, Paul Kennedy, Eric P. Achterberg, Andrew G. Dickson, Matthew Mowlem, Hilary Kennedy

PII: S0016-7037(17)30626-9
DOI: https://doi.org/10.1016/j.gca.2017.09.037
Reference: GCA 10489

To appear in: *Geochimica et Cosmochimica Acta*

Received Date: 21 April 2017
Accepted Date: 21 September 2017

Please cite this article as: Papadimitriou, S., Loucaides, S., Rérolle, V.M.C., Kennedy, P., Achterberg, E.P., Dickson, A.G., Mowlem, M., Kennedy, H., The stoichiometric dissociation constants of carbonic acid in seawater brines from 298 to 267 K, *Geochimica et Cosmochimica Acta* (2017), doi: https://doi.org/10.1016/j.gca.2017.09.037

The stoichiometric dissociation constants of carbonic acid in seawater brines from 298 to 267 K

Stathys Papadimitriou[a,*], Socratis Loucaides[b], Victoire M. C. Rérolle[b,1], Paul Kennedy[a], Eric P. Achterberg[c,2], Andrew G. Dickson[d], Matthew Mowlem[b], Hilary Kennedy[a]

[a]Ocean Sciences, College of Natural Sciences, Bangor University, Menai Bridge, Anglesey LL59 5AB, UK

[b]National Oceanography Centre, Southampton, SO14 3ZH, UK

[c]University of Southampton, National Oceanography Centre, Southampton, SO14 3ZH, UK

[d]Marine Physical Laboratory, Scripps Institution of Oceanography, University of California, San Diego, 9500 Gilman Drive, La Jolla, CA 92093-0244, USA

[1]Present address: FLUIDION SAS, 75001 Paris, France

[2]Present address: GEOMAR, Helmholtz Centre for Ocean Research, 24148 Kiel, Germany

[*]Corresponding author: s.papadimitriou@bangor.ac.uk (e-mail)

Abstract

The stoichiometric dissociation constants of carbonic acid (K^*_{1C} and K^*_{2C}) were determined by measurement of all four measurable parameters of the carbonate system (total alkalinity, total dissolved inorganic carbon, pH on the total proton scale, and CO_2 fugacity) in natural seawater and seawater-derived brines, with a major ion composition equivalent to that Reference Seawater, to practical salinity (S_P) 100 and from 25 °C to the freezing point of these solutions and –6 °C temperature minimum. These values, reported in the total proton scale, provide the first such determinations at below-zero temperatures and for $S_P > 50$. The temperature (T, in Kelvin) and S_P dependence of the current pK^*_{1C} and pK^*_{2C} (as negative common logarithms) within the salinity and temperature ranges of this study ($33 \leq S_P \leq 100$, $-6\ °C \leq t \leq 25\ °C$) is described by the following best-fit equations: $pK^*_{1C} = -176.48 + 6.14528\ S_P^{0.5} - 0.127714\ S_P + 7.396\times10^{-5}\ S_P^2 + (9914.37 - 622.886\ S_P^{0.5} + 29.714\ S_P)\ T^{-1} + (26.05129 - 0.666812\ S_P^{0.5})\ \ln T$ ($\sigma = 0.011$, $n = 62$), and $pK^*_{2C} = -323.52692 + 27.557655\ S_P^{0.5} + 0.154922\ S_P - 2.48396\times10^{-4}\ S_P^2 + (14763.287 - 1014.819\ S_P^{0.5} - 14.35223\ S_P)\ T^{-1} + (50.385807 - 4.4630415\ S_P^{0.5})\ \ln T$ ($\sigma = 0.020$, $n = 62$). These functions are suitable for application to investigations of the carbonate system of internal sea ice brines with a conservative major ion composition relative to that of Reference Seawater and within the temperature and salinity ranges of this study.

1. Introduction

The investigation of the carbonate system in aquatic environments is essential in the understanding and monitoring of the carbon cycle in the hydrosphere. Such investigations have intensified in the marine environment because of the crucial role the ocean plays in the absorption and storage of the anthropogenic CO_2 emitted to the atmosphere during the Industrial era (Takahashi et al., 1997; Sabine et al., 2004). Through this process, the ocean is a major repository of anthropogenic CO_2 (Takahashi, 2004), with consequent chemical and ecosystem functioning effects from the acidification of surface oceanic waters (decreased oceanic pH relative to pre-industrial era values) (Caldeira and Wickett, 2003; Feely et al., 2004; Takahashi et al., 2014; Gattuso et al., 2015). The acidification effect on the oceanic carbonate system by atmospheric CO_2 absorption (Takahashi, 2004; Sabine et al., 2004) has been observed in surface coastal and pelagic waters (Takahashi et al., 2014), including large areas of the Arctic Ocean (Feely et al., 2008; Yamamoto-Kawai et al., 2009; Cai et al., 2010; Semiletov et al., 2016).

One of the challenges that remain in the high latitude (polar) oceans of the Earth's cryosphere is reliable determination of the carbonate system in the brine-ice system in the extensive seasonal sea ice cover of these environments (Brown et al., 2014; Miller et al., 2015; Papadimitriou et al., 2016). Early investigations in the composition and activity of the ice-associated (sympagic) microbial community in sea ice have uncovered the role of this multi-phase system on the surface of high latitude oceans as a habitat akin to other large-scale biomes, such as the desserts and tundra (Fritsen et al., 1994; Gleitz et al., 1995; Arrigo et al., 1997; Thomas and Dieckmann, 2002; Kennedy et al., 2002). Subsequent investigations have revealed a complex internal carbon cycle driven not only by the sympagic autotrophic and heterotrophic microbial communities, but also by two other major chemical reactions in the surface ocean, CO_2 gas exchange and hydrated $CaCO_3$ authigenesis (Papadimitriou et al., 2004; Delille et al., 2007; Dieckmann et al., 2008; Munro et al., 2010; Papadimitriou et al., 2012; Fischer et al., 2013). The internal carbon cycling in sea ice is complemented by measurable CO_2 fluxes to and from the atmosphere as a function of ice temperature (Delille et al., 2014) and to the underlying ocean by gravity drainage of the internal brines (Rysgaard et al., 2007; Rysgaard et al., 2011). These past investigations have culminated in a keen interest in the carbonate system of sea ice brines (Brown et al., 2014; Miller et al., 2015), the residual internal solution where all biogeochemical reactions occur either in isolation from, or in direct exchange with, the adjacent seawater column and the atmosphere

depending on the temperature- and salinity-dependent permeability of the medium (Golden et al., 1998). Sea ice brines are derived from the frozen surface seawater by physical concentration of the dissolved sea solutes following their expulsion from the ice crystal matrix. Along with degassed components, the brines can become trapped in pockets and channels in the sea ice structure. As a result of internal thermal equilibrium in sea ice along temperature gradients extending seasonally slightly above or far below the freezing point of seawater (–1.92 °C at 0 dbar pressure and salinity 35; UNESCO, 1983), the salinity of internal brines can vary from the hyposaline to values in excess of 100 below –6 °C, and the concentration of brine solutes can likewise vary (Gleitz et al., 1995; Miller et al., 2011a, 2011b; Papadimitriou et al., 2012; Geilfus et al., 2012a).

The carbonate system in the marine environment is defined by pressure, temperature, salinity, the total concentration of boron and the dissociation constant of boric acid, the total concentrations of sulfate and fluoride, along with the equilibrium constants for the formation of the bisulfate ion and HF, respectively, the dissociation constants of carbonic acid, the value of two of its four measurable parameters [total alkalinity (A_T), total dissolved inorganic carbon (C_T), pH, and the fugacity of CO_2 (fCO_2)] and, lastly, the weak acid-base systems in the dissolved macro-nutrient and metabolite pools (phosphate, silicate, ammonium, sulphide) and their respective dissociation constants (Millero, 1995; Dickson et al., 2007). To date, all relevant dissociation constants have been adequately constrained empirically as a function of temperature and salinity for above-zero temperatures and practical salinity (S_P) up to 50 (Millero, 1995, and references there-in). Great investigative effort has been invested in the experimental determination of the first and second stoichiometric (concentration-based) dissociation constants of carbonic acid in seawater and solutions derived from seawater by dilution or evaporation, both in natural and artificial media with the mean stoichiometric composition of seawater (Hansson, 1973; Mehrbach et al., 1973; Goyet and Poisson, 1989; Roy et al., 1993; Mojica-Prieto and Millero, 2002; Millero et al., 2006). The determination of the carbonate system in the complex and sparsely accessible sea ice system is currently limited to direct measurements of A_T and C_T (Miller et al., 2015) and is further compounded by the large uncertainty in the values of the relevant acid-base dissociation constants as they are currently estimated via extrapolation of the existing different salinity-temperature functions to the physical sea ice conditions (temperature < 0 °C, $S_P > 50$) (Brown et al., 2014). Direct in-situ measurements of fCO_2 in the sea ice system are

still rare either in bulk sea ice (Miller et al., 2011a, b; Geilfus et al., 2012b) or in brines, which are, moreover, subject to the sparse spatial resolution afforded by brine collection in boreholes through the ice surface (Delille et al., 2007; Geilfus et al., 2012a; Delille et al., 2014). In addition, direct brine pH measurement has not been possible so far at below-zero temperatures and high salinities as a result of sampling and analytical difficulties in this complex system. As a first step towards the implementation of direct pH measurement in sea ice brines, the pH of Tris buffers (Papadimitriou et al., 2016) and the $p(K_2e_2)$ of the pH-indicator dye *meta*-Cresol Purple (Loucaides et al., 2017) have recently been characterized electrometrically with the Harned cell and spectrophotometrically, respectively, to $S_P = 100$ and –6 °C. Sea ice geochemists, therefore, have so far relied on indirect determination of brine fCO_2 and pH from the solution of the system of equations that describe the acid-base equilibria of the oceanic carbonate system using temperature, salinity, nutrient concentrations (if available), and the direct measurements of A_T and C_T as input parameters, with the caveats of extrapolation mentioned above (Brown et al., 2014).

Here, we present measurements that allowed the determination of the dissociation constants of carbonic acid in seawater and seawater-derived brines at below-zero temperatures to the freezing point of these solutions up to $S_P = 100$ and a temperature minimum of –6 °C. The S_P and temperature ranges of this study were set because the ionic composition and inter-ionic ratios in surface oceanic water are conserved in the natural sea ice brines over these temperature and salinity ranges. More concentrated, cooler sea ice brines ($S_P > 100$ and $t < –6$ °C) become supersaturated with respect to a suite of hydrated solid phases, including mirabilite, hydrohalite, and gypsum (Butler and Kennedy, 2015; Butler et al., 2016; Butler et al., 2017), thus altering the chemical composition and ionic ratios of the brines from those in surface oceanic water (Marion, 2001). Determination of equilibrium constants beyond the current salinity-temperature range must account for these compositional modifications (Hain et al., 2015) by solid-solution reactions, and so, it requires custom experimental protocols in a separate investigation.

2. Materials and Methods

The stoichiometric first (K_{1C}^*) and second (K_{2C}^*) dissociation constants of carbonic acid describe the equilibrium of the reactions, $CO_2^* + H_2O \leftrightarrow H^+ + HCO_3^-$ and $HCO_3^- \leftrightarrow H^+ + CO_3^{2-}$, respectively, with $[CO_2^*] = [CO_2(aq)] + [H_2CO_3]$ (Dickson et al., 2007). In this study, they were

determined in natural high ionic strength solutions (seawater, seawater-derived brines) from measurements of A_T, C_T, fCO_2, and $pH_T = -\log[H^+]_T$ (total proton scale) as follows (Millero et al., 2002):

$$K^*_{1C} = [H^+]_T \frac{2C_T - A_C - 2[CO^*_2]}{[CO^*_2]}, \quad (1)$$

$$K^*_{2C} = [H^+]_T \frac{A_C - C_T + [CO^*_2]}{2C_T - A_C - 2[CO^*_2]}, \quad (2)$$

In the above equations, A_C = carbonate alkalinity = $[HCO_3^-] + 2[CO_3^{2-}]$, $C_T = [CO^*_2] + [HCO_3^-] + [CO_3^{2-}]$, and $[CO^*_2] = K_o\, fCO_2$, with $K_o = CO_2$ solubility constant as a function of salinity and temperature (Weiss, 1974), and brackets denoting total concentrations (single ion plus ion pairs in the case of pair-forming ionic species).

Carbonate alkalinity was determined from the measured A_T and pH_T as described in Millero et al. (2002). To this end, the contributions of dissolved phosphate and silicic acid to A_T were computed from their measured total concentrations, the measured pH_T, and the relevant stoichiometric equilibrium dissociation constants computed from the available salinity-temperature functions (Millero, 1995; Dickson et al., 2007). For the contribution of boron alkalinity to A_T, the mean total boron concentration, $[B_T] = 0.000432578$ mol $kg^{-1}_{solution}$ (hereafter, mol kg^{-1}), in $S_P = 35$ seawater as computed from the data in Lee et al. (2010) was used as a linear function of salinity (Millero, 1995), along with the measured pH_T and the stoichiometric equilibrium dissociation constant of boric acid in Dickson (1990). The contributions to A_T of OH^- (positive), H^+ (total proton scale), and HF (both negative and negligible in the pH range of this study) were determined using the measured pH_T, the concentration of SO_4^{2-} and F^- in Reference Seawater as a linear function of salinity (Millero et al., 2008), and the relevant equilibrium constants from the available oceanographic functions (Millero, 1995; Dickson et al., 2007). The oceanographic functions for the equilibrium constants used for these computations were extrapolated outside their empirical salinity-temperature ranges ($t \geq 0$ °C, $S_P < 50$; Dickson, 1990; Millero, 1995) when the experimental conditions extended beyond them ($t \leq 0$ °C, $S_P > 50$). Locally sourced seawater (Menai Strait; 53.1806N 4.2333W), UV-sterilized and filtered through a 0.2 μm filter, was used as the experimental medium (S_P = 33 – 34) and for the

preparation of the experimental brines (S_P = 40 – 100) by variable freezing and gravimetric dilution, when needed, with ultrapure (18 MΩ·cm) Milli-Q™ water. The brines were filtered through pre-combusted (500 °C, 3 hrs) GF/F filters (0.7 μm, WHATMAN); they were then sampled for the determination of major ion concentrations (Na^+, K^+, Ca^{2+}, Mg^{2+}, Cl^- and Br^-, SO_4^{2-}) and were kept stored at room temperature in the dark in acid-washed glass media bottles (DURAN) capped (gas-tight) with Teflon-lined screw-caps.

The experiments were conducted at zero and below-zero temperatures to very near the freezing point of seawater and seawater-derived brines, as well as at above-zero temperatures to 25 °C, in order for our experimental results to span the existing data sets for the stoichiometric equilibrium dissociation constants of carbonic acid in natural seawater and brines for validation. The freezing point (t_{FP}, in °C) of the experimental brines was estimated from the empirical temperature function for the weight-based salinity (S_W, in g kg^{-1}) of thermally equilibrated sea ice brines, $S_W = 1000\ [1 - (54.11/t_{FP})]^{-1}$ (Assur, 1958). For S_W to S_P conversion, the recent absolute salinity (S_A) and (conductivity-based) S_P relationship, $S_A = 1.004715\ S_P$ (Millero and Huang, 2009), was used. The estimated t_{FP} was within ± 0.05 °C to –5 °C and –0.15 °C to –6 °C from the values computed from the S_P–t_{FP} standard oceanographic relationship for seawater in UNESCO (1983) extrapolated to $S_P > 40$.

Each salinity-temperature experiment was conducted with ~1.1 L seawater or brine in a Teflon-lined-capped media bottle (DURAN), which was thermally equilibrated by immersion in a thermostated ethylene-glycol/water bath (GRANT TX150) and was kept at constant temperature during measurement and sampling for the analysis of the required parameters. The experimental temperature was monitored with a Fluke 5609 Platinum Resistance Probe on a Hart Scientific 1502A Thermometer and is reported as the mean of the values recorded for the duration of each experiment. Throughout the experiment, the sample was gently stirred (50 rpm) with an overhead stainless steel stirrer through the cap. Each experiment required about 70 minutes to complete the necessary measurements (fCO_2 and pH_T) at the experimental temperature and the sample collection for the remainder of analyses. First, the fCO_2 and pH_T measurements were conducted simultaneously in separate aliquots of the sample, drawn through Tygon® tubings with a Watson Marlow 520U peristaltic pump towards the CO_2 Analyzer unit and the pH unit. Upon completion of these measurements, samples for C_T determination were pump-drawn and flame-sealed into pre-weighed 10 mL glass ampoules poisoned with saturated mercuric

chloride. Subsequently, samples for soluble reactive phosphorus (SRP, hereafter, phosphate) and molybdenum reactive silicon [hereafter, silicic acid, $Si(OH)_4$] were removed and the remaining sample was used for replicate A_T determinations.

2.1 fCO_2 measurement

The fCO_2 was determined from the CO_2 mole fraction (x_{CO_2}) measured on a LICOR 840A CO_2/H_2O analyzer of the dry gas generated in a closed loop by exchange with the sample via a 0.5×1 MicroModule^{TM} Membrane Contactor (Liqui-Cell; www.liquicell.com), used here as the gas exchange unit (Hales et al., 2004a). The gas was circulated in the closed loop at 48 mL min^{-1} through a custom-made DRIERITE desiccant column (www.drierite.com) with a custom-made gas micro-pump. The contactor was immersed in a custom-made housing in the same water bath as the sample, which was pumped through the contactor at 9 mL min^{-1} in Tygon® tubing via the Watson Marlow 520U peristaltic pump. The temperature of the sample in the bottle and at the exit of the contactor was monitored with type K thermocouple probes by continuous logging on a Pico Technology USB TC-08 thermocouple data logger. In this set-up, a plateau in x_{CO_2} was achieved in 50 min, and the x_{CO_2} used for fCO_2 determination in each thermostated sample was a 5 min average of recorded values within the plateau phase. These values were within 1 ppm for $x_{CO_2} < 1000$ ppm and within 3 ppm for $x_{CO_2} > 1000$ ppm. The measurements were calibrated against CO_2/N_2 mixtures with a certified x_{CO_2} (0, 20, 100, 400, 1000, and 2000 ppm; uncertainty ≤ 5%, BOC, boc.com). The calibrations were conducted between two consecutive experiments. The sample fCO_2 was computed from the measured x_{CO_2} as in SOP 5 in Dickson et al. (2007), using the pressure readings from the built-in barometer in the LICOR gas cell.

An estimate of the uncertainty of these measurements was possible at above-zero temperatures by analyzing, with this protocol, samples of CO_2 in Seawater Certified Reference Materials (CRM, Batches #112, #124, and #125; Scripps Institution of Oceanography) and comparing the measured fCO_2 with that computed from the certified C_T and A_T, as well as the salinity and the phosphate and silicic acid concentrations reported in the certificate. The CRM fCO_2 analyses were thus conducted every 1 – 4 °C in the temperature range from 3.16 °C to 24.99 °C (batch #112: n = 11; batch #124, n = 1; batch #125, n = 1). For the calculations, the first and second dissociation constants of carbonic acid were computed from the salinity-temperature

functions based on the measurements of Mehrbach et al. (1973) as refitted on the total proton scale by Lueker et al. (2000). The dissociation constants of the remainder of the weak acids and bases of the oceanic carbonate system, the solubility of CO_2 in seawater, and the B_T and the total dissolved sulphate and fluoride concentrations were computed as described earlier. All computations were conducted on the total proton scale by solving for pH the system of equations that describe the equilibria of the marine carbonate system using the Solver routine on Microsoft Excel. At the computed CRM fCO_2 from 225 µatm at 3.16 °C to 567 µatm at 24.99 °C for batch #112 and 537 µatm at 22.03°C for batch #124, the measured fCO_2 differed by (mean ± 1σ) –9 ± 10 µatm (n = 12). This estimated uncertainty is equivalent to –2 ± 3% relative to the computed fCO_2 and consists of the measurement uncertainty and the computational uncertainty. The computational uncertainty is due to the combined uncertainties in the certified parameters and in the acid-base dissociation constants used in the computations, including the uncertainty in pK^*_{1C} and pK^*_{2C} (0.0055 and 0.0100 pK unit, respectively; Lueker et al., 2000). Based on the assessment in Lueker et al. (2000), the computational fCO_2 uncertainty has been estimated to be 1.6% for the uncertainty in the certified A_T and C_T concentrations (3 µmol kg^{-1} for both A_T and C_T; Bockmon and Dickson, 2015). This indicates that the computational uncertainty was a significant contributor to the estimated uncertainty in the current methodology for up to 600 µatm fCO_2. The measured fCO_2 differed by –85 µatm at CRM fCO_2 = 1062 µatm at 18.06 °C for batch #125, equivalent to –8% relative to the computed fCO_2. In contrast, in the assessment of Lueker et al. (2000), the measured fCO_2 was systematically higher by +3.35 ± 1.22% than the computed fCO_2 at fCO_2 > 500 µatm. In comparison, the uncertainty based on the single high-fCO_2 CRM measurement (batch #125) available during this study suggests an increased negative bias at high fCO_2 (~ 1,000 µatm, or higher) with the current methodology.

2.2 pH measurement

The pH_T (total proton scale) was determined spectrophotometrically using purified *meta*-Cresol Purple (mCP) indicator dye, the salinity and temperature functions of its optical parameters and second stoichiometric equilibrium dissociation constant (on the total proton scale) as determined in the same temperature and salinity ranges as in this study by Loucaides et al. (2017), and the custom-made micro-opto-fluidic Lab-On-Chip (LOC) pH system described in Rérolle et al. (2013). The LOC unit with its sample and dye inlets, as well as the optics

(photodiode detector and light source) were all custom-housed and immersed as a separate micro-unit in the same thermostated water bath as the sample and the fCO_2 contactor described in the previous section. The electronics, pumps, and reagent stores were outside the water bath. The mCP solutions used in this study were prepared from the same batch of HPLC-purified dye that was used for the characterization of the dye as reported in Loucaides et al. (2017). The pH_T is reported as the mean of several injections (5 – 10) per sample through the LOC pH system. In the case of the pH_T measurements used in the determination of K^*_{1C} and K^*_{2C} (eqs. 1 and 2), these multiple injections occurred over the course of the simultaneous fCO_2 determination, with a reproducibility better than 0.004 pH unit (as 1σ). The uncertainty associated with the pH_T measurement protocol was assessed against the pH_T computed for CRMs as described in the previous section for fCO_2. The CRM pH analyses were thus conducted every 1 – 2 °C in the temperature range from 1.52 °C to 25.15 °C using CRM batches #112 (n = 5), #124 (n = 1), and #125 (n = 1), which were also used for the fCO_2 protocol validation described in the previous section, as well as batch #138 (n = 15), used here only for the validation of the pH measurement protocol. At the computed CRM pH_T for batches #112 (7.908 at 24.99 °C to 8.264 at 1.97 °C), #124 (7.927 at 22.03 °C), and #138 (7.852 at 25.15 °C to 8.215 at 1.52 °C), the measured pH_T differed by (mean ± 1σ) –0.013 ± 0.011 pH unit (n = 21). For the high-fCO_2 CRM batch #125 (CRM pH_T = 7.659 at 18.06 °C), the measured pH_T differed by +0.015 pH unit. Numerical evaluation yielded a computational uncertainty of ± 0.010 pH unit due to the combined uncertainties in the certified parameters (3 μmol kg^{-1} for both A_T and C_T; Bockmon and Dickson, 2015) and in the pK^*_{1C} and pK^*_{2C} (0.0055 and 0.0100 pK unit, respectively; Lueker et al., 2000) used in the computation of the CRM pH_T. This suggests that about half of the overall uncertainty evaluated on the CRM pH_T determinations (~ 0.020 pH unit as 2σ) can be attributable to computational uncertainty. A similar uncertainty of 0.010 – 0.020 pH unit was evaluated for the pH_T measurement on the same batch of purified mCP and analytical set-up throughout the current experimental temperature and salinity ranges by Loucaides et al. (2017) based on relevant, electrochemically characterized Tris-HCl buffer solutions (Papadimitriou et al., 2016).

2.3 A_T and C_T measurements

Total alkalinity was determined by open-cell potentiometric titration with 0.1 N HCl at 20 °C using the Gran function for pH < 3.5 (Gleitz et al., 1995; Papadimitriou et al., 2013) with a

Metrohm Titrando 888 unit of automatic burette, pH meter, Pt temperature probe, Ag/AgCl/KCl reference electrode, and glass indicator electrode calibrated with buffers traceable to SRM from NIST and PTB (Merck, pH 2.00, 4.01, 7.00, 9.00, and 10.00 at 25 °C). The titration was conducted in replicate ~100 mL aliquots of known weight at constant pCO_2 (400 ppm CO_2) provided at a controlled rate (200 mL min^{-1}) via a CHELL CMD100 microprocessor controller and Hastings Mass Flow Control Valve. The rigour of the technique was assessed from several titrations of CRM batch #112 (A_T = 2223.26 μmol kg^{-1}) with a coulometry-characterized HCl solution (0.100171 mol HCl kg^{-1}, ~0.7 M NaCl; Scripps Institution of Oceanography), yielding a difference of measured from certified A_T of –1.9 ± 1.7 μmol kg^{-1} (n = 23), equivalent to 0.08% reproducibility and accuracy. Batches of 0.1 N HCl were also prepared gravimetrically in the course of this study to a total ionic strength of 0.72 molal using NaCl, and the HCl concentration was calibrated against the A_T of CRM batches #112 and #138. The difference between the A_T measured with these acid batches and the certified concentrations was –1.1 ± 2.8 μmol kg^{-1} (n = 99) in good agreement with that determined with the Scripps CRM and acid. Because the acid batches were calibrated against seawater CRMs and the response of commercial glass electrodes may be unreliable in hypersaline solutions, the A_T in brines was determined in samples diluted gravimetrically to a salinity of 34 with ultrapure (18 MΩ·cm) Milli-Q™ water. The A_T of the brine batches (Table 2), normalized to salinity 35, was $A_{T,35}$ = 2424 ± 39 μmol kg^{-1} (n = 10), while the local seawater had a two-year (2014-2015) average $A_{T,35}$ = 2398 ± 22 μmol kg^{-1} (n = 37).

The C_T concentration was determined manometrically in 3 – 10 replicate sample aliquots (~10 mL) from the CO_2 generated and extracted in vacuo in a glass manifold following reaction of a weighed sample aliquot with H_3PO_4 and cryogenic CO_2 gas distillation in successive cold (–95 ºC) methanol and liquid nitrogen traps, using an in-line manometer (CHELL) and a virial equation of state (Bockmon and Dickson, 2015). The reproducibility of these measurements was better than 0.4% in the 2000 to 5600 μmol kg^{-1} concentration range. Determination of C_T on CRM batches #112, #124, #125, and #138 (Scripps Institution of Oceanography) yielded a difference between the measured and certified C_T of (mean ± 1σ) +0.7 ± 8.8 μmol kg^{-1} (n = 111).

2.4 Other measurements

The salinity of the experimental solutions was measured at laboratory temperature (~20 ºC) using a portable conductivity meter (WTW Cond 3110) with a WTW Tetracon 325 probe. When salinities exceeded 70, they were determined following gravimetric dilution with distilled water. The initial major ion composition of the brines was determined as follows: (*i*) potentiometric titration with EDTA as titrant and Tris-buffered acetylacetone (0.1 M) as the complexing agent at pH ~8.5 for Ca^{2+} and Mg^{2+} as described in Papadimitriou et al. (2012), (*ii*) ion chromatography on a Dionex Ion Exchange Chromatograph ICS 2100 for Na^+ and K^+, (*iii*) gravimetric Mohr titration for total halides (except F^-, but mostly Cl^-, with comparatively small contributions from bromide and smaller by iodine; hereafter termed: $[Cl^-] + [Br^-]$) with 0.3 mol kg^{-1} $AgNO_3$ standardized against NaCl purified by re-crystallization (Dickson, 1990; Millero et al., 1993), and (iv) for SO_4^{2-}, precipitation as $BaSO_4$ in EDTA followed by titration with $MgCl_2$ (Howarth, 1978). The phosphate and silicic acid concentrations were determined within 4 to 8 weeks from collection on refrigerated aliquots stored in acid-washed (2 N HCl) 20 mL PE vials. These analyses were conducted on a SEAL AA3 MR continuous segmented flow autoanalyzer using standard colorimetric methodology (Hales et al., 2004b).

2.5 Error analysis

The error in the experimental K_{1C}^* and K_{2C}^* values was computed as $\sigma^2_{K^*_{iC}} = \sum[(dK^*_{iC}/dX)\,\sigma_X]^2$ (Barford 1985), with X = H^+, C_T, A_C, CO_2(aq) (all in mol kg^{-1}). The maximum measurement uncertainty (σ_X) was 0.020 pH unit for the pH measurements, 0.4% for the C_T determinations, 20 µatm for fCO_2 < 1000 µatm, 90 µatm for fCO_2 > 1000 µatm, and 0.1% for the A_C estimates based on the uncertainty of the A_T measurement. The magnitude of the extrapolation error for the estimates of the non-carbonate A_T components is unknown at this stage. The available measurement uncertainties in pH_T, C_T, fCO_2, and A_C determinations indicated that K_{1C}^* is most sensitive to uncertainties in the pH and fCO_2 measurements, while K_{2C}^* is most sensitive to the uncertainties in the A_C estimates and the C_T and pH measurements. The K_{1C}^* uncertainty was thus calculated to range from 0.020 – 0.040 pK unit at fCO_2 > 250 µatm to 0.050 pK unit at fCO_2 < 250 µatm. The K_{2C}^* uncertainty was calculated to be 0.040 pK unit for our experiments. The uncertainties of both constants in this study are therefore estimated to be about twice those

reported for standard oceanographic conditions (0.020 pK unit for K^*_{1C} and 0.030 pK unit for K^*_{2C}; Dickson and Millero, 1987).

2.6 Data evaluation

The K^*_{1C} and K^*_{2C} determinations in seawater at above-zero temperatures were evaluated against the existing major data sets in natural seawater, i.e., the Mehrbach et al. (1973) data set (experimental ranges: S_P = 19 – 43, t = 2 – 35 °C) as refitted on the total proton scale by Lueker et al. (2000) and the Millero et al. (2006) data set (experimental ranges: S_P = 1 – 51, t = 1.0 – 50.5 °C). Because the latter data set has been reported on the seawater proton scale, it was converted to the total proton scale as described in Millero (1995) and was re-fitted here using the same equation format as in the original study:

$$pK^*_{iC} = pK^o_{iC} + A_i + B_i/T + C_i \ln T \ (i = 1, 2), \quad (3)$$

In the above equation, T = temperature (in Kelvin), $A_i = a_o S_P^{0.5} + a_1 S_P + a_2 S_P^2$, $B_i = a_3 S_P^{0.5} + a_4 S_P$, $C_i = a_5 S_P^{0.5}$, and $pK^o_{iC} = b_o + b_1/T + b_2 \ln T$ = thermodynamic equilibrium dissociation constant, with a_o, a_1, a_2, a_3, a_4, a_5 = best-fit parameters (Table 3) determined by non-linear regression using the Excel regression routine, while b_o, b_1, and b_3 are from Millero et al. (2006). The standard error of the fit was the same as in the original study ($\sigma_{pK^*_{1C}}$ = 0.006 and $\sigma_{pK^*_{2C}}$ = 0.011).

The current pK^*_{1C} and pK^*_{2C} determinations in natural seawater (S_P = 33 – 34; mean S_P = 33.66 ± 0.36, n = 5) over the temperature range from 0 to 25 °C (Table 2) are in very good agreement with the previously published data sets (Fig. 1). Specifically, in the 0 – 25 °C temperature range, the current observations (n = 23) differed by ΔpK^*_{1C} = –0.009 ± 0.016 and ΔpK^*_{2C} = +0.002 ± 0.018 relative to the Mehrbach et al. (1973) data set, and ΔpK^*_{1C} = –0.014 ± 0.016 and ΔpK^*_{2C} = –0.003 ± 0.022 relative to the Millero et al. (2006) data set, all within experimental error. The determinations beyond the salinity-temperature bounds of the available oceanographic data sets (t < 0 °C, S_P > 50) were compared with the extrapolated values of the oceanographic equations as will be discussed in the *sections 3* and *4*. In addition, the K^*_{1C} and

K^*_{2C} determinations near the freezing point of seawater and seawater-derived brines from this study were compared with the values calculated from appropriate thermodynamic data as follows. Stoichiometric equilibrium constants are related to the thermodynamic equilibrium constants at infinite dilution (pure water) via the activity coefficients of the reacting ions. In the case of K^*_{1C} and K^*_{2C}, this relationship is given by the following equations (Millero et al., 2006):

$$K^*_{1C} = K^o_{1C} \frac{\gamma_{CO_2} \alpha_{H_2O}}{\gamma_{H^+} \gamma_{HCO_3^-}} \Theta, \quad (4)$$

$$K^*_{2C} = K^o_{2C} \frac{\gamma_{HCO_3^-}}{\gamma_{H^+} \gamma_{CO_3^{2-}}} \Theta, \quad (5)$$

where K^o_{1C}, K^o_{2C} = thermodynamic equilibrium dissociation constants of carbonic acid, α_{H_2O} = activity of water, γ_i = total ion activity coefficient (i = CO_2(aq), H^+, HCO_3^-, CO_3^{2-}) (in mol $kg^{-1}_{H_2O}$), and $\Theta = 1 - 0.001005\ S_P$ = conversion factor from mol $kg^{-1}_{H_2O}$ to mol $kg^{-1}_{solution}$ (Millero, 1995). For the calculation of the required thermodynamic equilibrium dissociation constants, α_{H_2O}, and γ_i at below-zero temperatures, the database of the FREZCHEM code (version 15.1) was used here, which is frequently used to examine geochemical processes in the cryosphere and is based on the Pitzer formalism of ionic interactions in strong electrolyte solutions (Marion, 2001; Marion et al., 2010). The FREZCHEM v15.1 includes some of the equilibria of the aqueous carbonate system (boron and fluoride chemistry, $CaCO_3$-solution equilibrium) and is rooted in the extant above-zero temperature data of the relevant thermodynamic equilibrium constants and Pitzer coefficients, with additional validation at below-zero temperatures from the metal-carbonate solubility data of the early 20th century Russian literature mostly at the eutectic point of these salt solutions (Marion, 2001). The model was run in the freezing mode (ice-water equilibrium) at 0.1 °C steps from 0 to –6 °C at 1 atm and a fixed pCO_2 at 400 μatm (non-conservative C_T) for a starting ionic composition equivalent to the composition of Reference Seawater of salinity 35 (Millero et al., 2008), with all other solid phases disabled (conservative major ionic composition and A_T). Total ion activity coefficients are directly proportional to the free ion activity coefficients, with the concentration ratio of the free ion to the sum of the free ion

and ion pairs as the proportionality factor (Pytkowicz and Kester, 1969). In the case of the total proton scale used in this study, $\gamma_{H^+} = \gamma_{H^+,free}\ m_{H^+,free} / (m_{H^+,free} + m_{HSO_4^-})$ (Millero, 1995), with m = molality (in mol $kg^{-1}_{H_2O}$) and all quantities in the right side of this equation obtained from the output of the code. The FREZCHEM code output provides the ionic strength (*I*) of model brines, and their S_P was estimated from the relationship, $I = 19.924\ S_P / (1000 - 1.005\ S_P)$ (Dickson et al. 2007). The code also computes α_{H_2O}, γ_{CO_2}, and the single ion activity coefficients of HCO_3^- and CO_3^{2-} from the Pitzer equations (Pitzer, 1973) and relevant Pitzer parameters. All ion pairs for HCO_3^- are considered adequately represented in the Pitzer computation (He and Morse, 1993) and so, the single ion activity coefficient of HCO_3^- in the code output is equivalent to $\gamma_{HCO_3^-}$ in eqs. (3) and (4). The code takes into account explicitly ion pair formation for CO_3^{2-} in the form of $CaCO_3^o$ and $MgCO_3^o$ (He and Morse, 1993; Marion, 2001). The molalities of these ion pairs were taken into account along with the molality and activity coefficient of CO_3^{2-} as a single ion in the code output to compute the total activity coefficient of CO_3^{2-} ($\gamma_{CO_3^{2-}}$) for use in eqs. (3) and (4) by applying the same principle as outlined above for γ_{H^+}.

2.7 Application to sea ice brines

A simple numerical model was used to illustrate the changes in the parameters of the carbonate system in seawater-derived brines with (*i*) conservative major ionic composition, A_T, and C_T, and (*ii*) brines of otherwise conservative chemical composition but at constant fCO_2 and, hence, non-conservative C_T, such as that which will occur as a result of dissolved-gaseous CO_2 exchange to atmospheric equilibrium. These scenarios are chosen for their simplicity for illustration purposes and cannot reflect the complexity of the carbonate system in sea ice brines as it is driven by several internal brine reactions at different and varying rates (Papadimitriou et al., 2004; Papadimitriou et al., 2007; Delille et al., 2007; Dieckmann et al., 2008; Munro et al., 2010; Geilfus et al., 2012a; Papadimitriou et al., 2012; Delille et al., 2014). The model was described in detail in Papadimitriou et al. (2014); briefly, it uses as a system of equations the weak acid-base equilibria in seawater, the salinity-normalized measured concentrations of phosphate, $Si(OH)_4$, C_T, and A_T in surface waters of the seasonal sea ice zone (SIZ) in the

western Weddell Sea, Antarctica, reported in Papadimitriou et al. (2012), along with the concentrations of SO_4^{2-} and F^- in Reference Seawater (Millero et al., 2008) and the mean total boron concentration in oceanic waters from Lee et al. (2010). In scenario (*i*) above, all these concentrations are conserved as a linear function of salinity, and the set of equations is solved for pH_T from A_T and C_T at each salinity-temperature pair at the freezing point of brines, allowing computation of the C_T speciation. In scenario (*ii*) above, all concentrations are conserved except C_T, and the system is solved for pH_T from fCO_2 and A_T, yielding C_T and its speciation. In this case, the fCO_2 was set at a constant value computed for 1 atm total pressure as described in Pierrot et al. (2009) from the average 2015 atmospheric CO_2 molar ratio (www.esrl.noaa.gov/gmd/ccgg/trends/). These calculations were done using the K_{1C}^* and K_{2C}^* determined in this study, as well as the values computed by extrapolation beyond their salinity maximum and temperature minimum of the salinity-temperature oceanographic functions described in the previous section.

3. Results

The initial composition of the brines for all major ions (Table 1), normalized to salinity 35, was in very good agreement with that of Reference Seawater (Millero et al. (2008) except for K^+, which was less by 1 mmol kg^{-1} on average, likely as a result of shading of the K^+ peak by the much greater Na^+ peak during ion chromatographic analysis. The conservative composition of the brines relative to that of Reference Seawater indicates no measurable alteration due to production of authigenic $CaCO_3$, $CaSO_4$, or Na_2SO_4 polymorphs over the short time scales of variable freezing of the seawater (6 – 15 hours) used here for brine preparation. It also justifies the use of the ionic composition of Reference Seawater in the thermodynamic evaluation of the current determinations of the stoichiometric equilibrium dissociation constants of carbonic acid.

The measured parameters and the determined stoichiometric equilibrium dissociation constants of carbonic acid (as negative common logarithms, pK_{1C}^* and pK_{2C}^*) are given in Table 2, with pK_{1C}^* and pK_{2C}^* reported in the total proton scale of the pH measurements. In the narrow below-zero temperature range to the freezing point of seawater [for the seawater S_P range from 33.14 to 34.04 used in this study (Table 2), t_{FP} = –1.82°C to –1.87°C (UNESCO, 1983)], the current observations (n = 6) were systematically higher than, but within experimental error from,

the values determined by below-zero temperature extrapolation of the best-fit curves on the existing data sets, with an overall ΔpK^*_{1C} = +0.015 ± 0.005 and ΔpK^*_{2C} = +0.019 ± 0.015 relative to both the Mehrbach et al. (1973) and Millero et al. (2006) data sets (Fig. 1). The measurements from natural brines (Table 2) from S_P = 40 to S_P = 100 and from 25 °C to near their freezing point (from –2.1 °C at S_P = 40 to –6.0 °C at S_P = 100) demonstrate that the determined pK^*_{1C} and pK^*_{2C} at S_P > 60 differ substantially at all temperatures from the values derived from the extrapolation of the existing oceanographic salinity-temperature functions (Fig. 2). Specifically, the current values are between the extrapolated values derived from the two oceanographic data sets used here for comparison. The greatest differences between measured and extrapolated values were seen at the highest salinities in the pK^*_{2C} relative to the best-fit equation derived from the Millero et al. (2006) data set, with ΔpK^*_{2C} = +0.72 ± 0.09 (n = 5) and +1.26 ± 0.12 (n = 6) at S_P = 85 and S_P = 100, respectively. For comparison, the equivalent ΔpK^*_{1C} was +0.13 ± 0.04 and +0.24 ± 0.07 at S_P = 85 and S_P = 100, respectively. The difference between the current and extrapolated values derived from the best fits to the Mehrbach et al. (1973) data set were similar for both pK^*_{1C} and pK^*_{2C} at the highest salinities (Fig. 2) and were more modest than those from the extrapolation of the Millero et al. (2006) data set, with ΔpK^*_{1C} = –0.19 ± 0.02 and ΔpK^*_{2C} = –0.12 ± 0.02 (n = 5) at S_P = 85 and ΔpK^*_{1C} = –0.32 ± 0.05, ΔpK^*_{2C} = –0.21 ± 0.04 (n = 6) at S_P = 100.

4. Discussion

4.1. The stoichiometric equilibrium dissociation constants of carbonic acid

It is of note that pK^*_{2C} changed more dramatically (over 0.4 pK unit) than pK^*_{1C} (over 0.1 pK unit) as a function of salinity at all temperatures in the current experiments (Fig. 2). The pK^*_{1C} computed from the output of the FREZCHEM thermodynamic code for the ionic composition of Reference Seawater at ice-water equilibrium was in excellent agreement with the current freezing point observations (Fig. 3). According to eq. (4), this indicates that all relevant thermodynamic parameters (K^o_{1C}, γ_{CO_2}, $\gamma_{HCO_3^-}$, γ_{H^+} and α_{H_2O}) are predicted reliably by the FREZCHEM code in the temperature range from the freezing point of seawater to that of S_P = 100 seawater-derived brine: K^o_{1C}, γ_{CO_2}, and $\gamma_{HCO_3^-}$ via extrapolation of the relevant above-zero temperature data sets of

He and Morse (1993) and Plummer and Busenberg (1982), γ_{H^+} from the Pitzer parameters for the specific interaction of the proton with all other ions in the model solutions, and α_{H_2O} from the Pitzer parameterization of the osmotic coefficient. This was not the case, however, for pK^*_{2C}, with differences up to 0.2 pK unit between current determinations and FREZCHEM-derived values (Fig. 3), which is higher than experimental uncertainty. A similar discrepancy trend was observed in the study of the stoichiometric equilibrium solubility product of ikaite in Papadimitriou et al. (2013). The current pK^*_{2C} determinations are based on the A_C estimated from the measured pH_T and A_T, and are, therefore, affected by the (unknown) extrapolation error for the estimates of the non-carbonate A_T components (section 2). However, the FREZCHEM-derived values are also affected by the same extrapolation error, which thus cannot exclusively explain the discrepancy between the current pK^*_{2C} determinations and the FREZCHEM-derived values. Based on eqs. (4) and (5), the disagreement in pK^*_{2C} with the thermodynamic code suggests uncertainty in K^o_{2C} or the total activity coefficient of CO_3^{2-}, or both, at below-zero temperatures. The total activity coefficient of CO_3^{2-} depends strongly on the extent of ion pair formation in solution. Its ion pairs with Ca^{2+} and Mg^{2+} have large equilibrium association constants which have to be taken into account explicitly in Pitzer parameterization routines, such as FREZCHEM, to complement the formal Pitzer parameterization of the CO_3^{2-} interactions in multi-electrolyte solutions (He and Morse, 1993; Marion, 2001). Knowledge about the behaviour of these strong ion pairs is based on the above-zero temperature study of Plummer and Busenberg (1982), while the Pitzer parameters for the single ion activity coefficient of CO_3^{2-} are based on the above-zero temperature experiments of He and Morse (1993). It is conceivable that targeted relevant experiments that will expand the empirical thermodynamic data base for the C_T species to below-zero temperatures may reconcile such differences as that seen here with respect to CO_3^{2-} (Fig. 3). This is in line with the objectives of the recent SCOR Working Group 145 for the update of chemical speciation modelling in seawater (Turner et al., 2016).

The pK^*_{1C} and pK^*_{2C} values determined in this study were fitted to the same equation format (eq. 3) as described in *Section 2.6*, and the best-fit coefficients are given in Table 3. The standard error of the fit was $\sigma_{pK^*_{1C}} = 0.011$ and $\sigma_{pK^*_{2C}} = 0.020$, and the fitted residuals demonstrated no

significant trends as a function of salinity and temperature (Fig. 4). These equations are suitable for interpolation within the salinity and temperature ranges of this investigation ($33 \leq S_P \leq 100$, $-6\ °C \leq t \leq 25\ °C$), but not outside these ranges, in conservative seawater-derived brines only. Specifically, they are relevant to solutions with the composition of Reference Seawater (Table 1) and the conservative-composition brines that can be derived from it. By altering the free-ion and total-ion activity coefficients, solution composition changes can affect the value of stoichiometric equilibrium constants as a function of ionic strength relative to the temperature-dependent thermodynamic value of said constants at constant temperature [e.g., He and Morse (1993) for pK_{1C}^* and pK_{2C}^* at above-zero temperatures in NaCl, Mg-Na-Cl, and Na-SO_4-Cl solutions to 6 m]. Assessment of solution composition is, therefore, the first step for rigorous use of available empirical stoichiometric equilibrium constants. More specifically, the current empirical salinity and temperature functions of pK_{1C}^* and pK_{2C}^* (Table 3) are not recommended for extrapolation in the hyposaline and more hypersaline regions of the salinity spectrum in sea ice, not least because, at the coldest part of sea ice temperature ($t < -6$ °C) where $S_P > 100$, the brine inclusions will have non-conservative ionic composition and altered major ionic ratios as a result of reactions with authigenic ikaite, mirabilite, gypsum, and hydrohalite (Papadimitriou et al., 2013; Butler and Kennedy, 2015; Butler et al., 2016; Butler et al., 2017). This will affect the value of stoichiometric equilibrium constants (Hain et al., 2015), which must be determined in the context of authigenic mineral-brine equilibria.

4.2. The carbonate system in sea ice

The simple numerical model described in *Section 2.7* was used to compute the change in pH_T, fCO_2, and CO_3^{2-} with decreasing temperature from the freezing point of S = 35 seawater to –6 °C ($S_P = 100$) in sea ice brines (Fig. 5). In brines which are conservative with respect to major ionic composition, A_T, and C_T, the pK_{1C}^* and pK_{2C}^* equations derived in this study predict a monotonic decrease in the pH_T from 8.03 to 7.86 coupled with increase in both the internal brine fCO_2 from 429 to 2262 µatm and the CO_3^{2-} concentration from 84 to 330 µmol kg^{-1}. These changes are anticipated solely from the physical concentration during the expulsion of seawater solutes from the ice crystal matrix in the process of sea ice formation and further cooling to –6 °C. If gas exchange occurs during seawater freezing and cooling of the sea ice system with all major ions

and A_T conserved in the internal brines, the composition of the brines is non-conservative with respect to C_T and, as a result, the brine fCO_2 is controlled by its equilibrium solubility. In this case, if atmospheric equilibrium is achieved in the brines, the brine pH_T is predicted to increase from 8.06 to 8.48 and the CO_3^{2-} concentration will also increase but to a much larger extent from 89 to 1017 μmol kg^{-1}.

The advantage gained by the current K_{1C}^* and K_{2C}^* data set relative to the extrapolation of the oceanographic equations parameterized for above-zero temperatures and $S_P < 50$ is evident in the difference in absolute values for all parameters concerned here. Of the two major oceanographic data sets used here for comparison, the extrapolation of the equations based on the Mehrbach et al. (1973) data set yielded the smallest such differences (Fig. 5), especially with respect to CO_3^{2-} in the conservative brine scenario (mean difference: –0.2 ± 3.8 μmol kg^{-1}) over the temperature range of the simulation (Fig. 5c). At the temperature minimum of this study and depending on the set of extrapolated oceanographic pK_{1C}^* and pK_{2C}^* equations, these differences were calculated to be up to +0.9 pH unit and –6000 μatm fCO_2 in the conservative brine C_T scenario (Figs. 5a-c), as well as up to –1300 μmol CO_3^{2-} kg^{-1} in the non-conservative brine C_T scenario (Fig. 5f). Similar differences have been reported as perplexing uncertainties of extrapolation in the sensitivity analysis for the sea ice brine carbonate system within $S_P = 50 – 70$ in Brown et al. (2014). The differences between the current and the two sets of extrapolated oceanographic pK_{1C}^* and pK_{2C}^* equations in respect of pH_T and fCO_2 computations at the freezing point for the conservative brine C_T scenario (Fig. 5a, b) can be coupled with the differences between measured pH_T and fCO_2 near the freezing point of experimental brines and their values derived from the relevant A_T and C_T measurements (Table 2) as computed using the two sets of extrapolated oceanographic pK_{1C}^* and pK_{2C}^* equations (Lueker et al., 2000; Millero et al., 2006). These are illustrated as a function of the C_T to A_T ratio (C_T/A_T) of the brine system (Fig. 6) and are increasingly significant at $S_P > 60$, higher C_T/A_T at constant t_{FP}–S_P, and, also, when the salinity- and temperature-extrapolated pK_{1C}^* and pK_{2C}^* equations in Millero et al. (2006) are used. The above comparisons (Figures 5 and 6) highlight the importance of re-evaluating the coefficients of the existing salinity-temperature functions on empirical data when applied to extended conditions.

Direct measurements at below-zero temperatures are rare for fCO_2 in sea ice brines (Delille et al., 2007; Geilfus et al., 2012a; Delille et al., 2014) or bulk sea ice (Miller et al., 2011a, b; Geilfus et al., 2012b) and have not been possible until recently for pH (Loucaides et al., 2017) due to sampling and analytical difficulties in this complex medium. Sea ice geochemists thus far have often relied on indirect determination of brine fCO_2 and pH in sea ice from direct measurements of A_T and C_T to determine the brine carbonate system, with the caveats of extrapolation (Brown et al., 2014), in order to assess the inorganic carbon budget in sea ice (Papadimitriou et al., 2007; Delille et al., 2007; Munro et al., 2010; Fransson et al., 2011; Geilfus et al., 2012a; Papadimitriou et al., 2012). The results of this study will provide confidence in the output of indirect parameter determination for the carbonate system in the below-zero temperature range in high salinity brines in parts of sea ice that are still warm enough to allow exchange with the air and the ocean. Additional studies are still required to extend the current empirical data base of the equilibrium dissociation constants of carbonic acid to the coldest temperature spectrum of sea ice to the eutectic and, also, to determine the behavior of the remainder weak acids and bases of the carbonate system in the full salinity and temperature spectrum of sea ice brines.

5. Conclusions

The stoichiometric equilibrium dissociation constants of carbonic acid determined in this study extended the existing oceanographic data set to below-zero temperatures and salinities greater than 50 to the freezing point of salinity 100 brines with major ionic composition and major ionic ratios equivalent to those of Reference Seawater. They are reported here in the total proton scale and each was fitted to a salinity and temperature function for interpolation in sea ice brine investigations of the internal carbonate system of the medium. This work confirmed the uncertainties of the salinity and temperature extrapolation of the existing oceanographic functions for application outside their empirical ranges. There were also indications for uncertainty in the current state of knowledge of the thermodynamic parameters (e.g., total activity coefficient of the carbonate ion) for the second equilibrium dissociation constant of carbonic acid at below-zero temperatures. Further relevant work is thus needed for accurate parameterization of the carbonate ion interactions with the remainder of sea solutes in brines at below-zero temperatures and for the dissociation constants of carbonic acid in the coldest temperature and salinity range of non-

conservative oceanic brines at equilibrium with authigenic cryogenic minerals to the eutectic of seawater.

Acknowledgements

This work was supported by a NERC-UK grant (grant NE/J011096/1). We thank Susan Allender for the dissolved macro-nutrient analyses and Dr. Ben Butler for the analyses of the major ions in the experimental solutions. We also thank three anonymous reviewers for their supportive and insightful comments.

References

Arrigo K. R., Worthen D. L., Lizotte M. P., Dixon P. and Dieckmann G. S. (1997) Primary production in Antarctic sea ice. *Science* **276**, 394-397.

Assur A. (1958) Composition of sea ice and its tensile strength in Arctic sea ice. U. S. National Academy of Sciences, National Research Council, Publ. 598, 106-138.

Barford N. C. (1985) Experimental measurements: Precision, error, and truth. John Wiley & Sons, Chichester, UK.

Bockmon E. E. and Dickson A. G. (2015) An inter-laboratory comparison assessing the quality of seawater carbon dioxide measurements. *Mar. Chem.* **171**, 36-43.

Brown K. A., Miller L. A., Davelaar M., Francois R. and Tortell P.D. (2014) Over-determination of the carbonate system in natural sea-ice brine and assessment of carbonic acid dissociation constants under low temperature, high salinity conditions. *Mar. Chem.* **165**, 36-45.

Butler B. M. and Kennedy H. (2015) An investigation of mineral dynamics in frozen seawater brines by direct measurement with synchrotron X-ray powder diffraction. *J. Geophys. Res. Oceans* **120**, 5686-5697, doi:10.1002/2015JC011032.

Butler B. M., Papadimitriou S., Santoro A., Kennedy H. (2016) Mirabilite solubility in equilibrium sea ice brines. *Geochim. Cosmochim. Acta* **182**, 40-54.

Butler B. M., Papadimitriou S., Day S. J., Kennedy H. (2017) Gypsum and hydrohalite dynamics in sea ice brines. *Geochim. Cosmochim. Acta* **213**, 17-34.

Cai W.-J., Chen L., Chen B., Gao Z., Lee S. H., Chen J., Pierrot D., Sullivan K., Wang Y., Hu X., Huang W.-J., Zhang Y., Xu S., Murata A., Grebmeier J. M., Jones E. P. and Zhang H. (2010) *Science* **329**, 556-559.

Caldeira K. and Wickett M. E. (2003) Anthropogenic carbon and ocean pH. *Nature* **425**, 365.

Delille B., Jourdain B., Borges A. V., Tison J.-L. and Delille D. (2007) Biogas (CO_2, O_2, dimethylsulfide) dynamics in spring Antarctic fast ice. *Limnol. Oceanogr.* **52**, 1367-1379.

Delille B., Vancoppenolle M., Geilfus N.-X., Tilbrook B., Lannuzel D., Schoemann V., Becquevort S., Carnat G., Delille D., Lancelot C., Chou L., Dieckmann G. S. and Tison J.-L. (2014) Southern ocean CO_2 sink: The contribution of the sea ice. *J. Geophys. Res. Oceans* **119**, 6340-6355.

Dickson A. G. (1990) Thermodynamics of the dissociation of boric acid in synthetic seawater from 273.15 to 318.15 K. *Deep-Sea Res.* **37**, 755-766.

Dickson A. G. and Millero F. J. (1987) A comparison of the equilibrium constants for the dissociation of carbonic acid in seawater media. *Deep-Sea Res.* **34**, 1733-1743.

Dickson A. G., Sabine C. L. and Christian J. R. (Eds.) (2007) Guide to best practices for ocean CO_2 measurements. PICES Special Publication 3, 191 pp.

Dieckmann G. S., Nehrke G., Papadimitriou S., Göttlicher J., Steininger R., Kennedy H., Wolf-Gladrow D. and Thomas D. N. (2008) Calcium carbonate as ikaite crystals in Antarctic sea ice. *Geophys. Res. Lett.* **35**, L08501, doi:10.1029/2008GL033540.

Feely R. A., Sabine C. L., Lee K., Berelson W., Kleypas J., Fabry V. J., Millero F. J. (2004) Impact of anthropogenic CO_2 on the $CaCO_3$ system in the oceans. *Science* **305**, 362-366.

Feely R. A., Sabine C. L., Hernandez-Ayon J. M., Janson D. and Hales B. (2008) Evidence for upwelling of corrosive "acidified" water onto the continental shelf. *Science* **320**, 1490-1492.

Fischer M., Thomas D. N., Krell A., Nehrke G., Göttlicher J., Norman L., Meiners K. M., Riaux-Gobin C. and Dieckmann G. S. (2013) Quantification of ikaite in Antarctic sea ice. *Antarct. Sci.* **25**, 421-432.

Fransson A., Chierici M., Yager P. L. and Smith Jr. W. O. (2011) Antarctic sea ice carbon dioxide system and controls. *J. Geophys. Res.* **116**, C12035, doi:10.1029/2010JC006844.

Fritsen C. H., Lytle V. I., Ackley S. F. and Sullivan C. W. (1994) Autumn bloom of Antarctic pack–ice algae. *Science* **266**,782-784.

Gattuso J.-P., Magnan A., Billé R., Cheung W. W. L., Howes E. L., Joos F., Allemand D., Bopp L., Cooley S. R., Eakin C. M., Hoegh-Guldberg O., Kelly R. P., Pörtner H.-O., Rogers A. D., Baxter J. M., Laffoley D., Osborn D., Rankovic A., Rochette J., Sumaila U. R., Treyer S. and

Turley C. (2015) Contrasting futures for ocean and society from different anthropogenic CO_2 emissions scenarios. *Science* **349**, 45, http://dx.doi.org/10.1126/science.aac4722.

Geilfus N. X., Carnat G., Papakyriakou T. N., Tison J.-L., Else B., Thomas H., Shadwick E. and Delille B. (2012a) Dynamics of pCO_2 and related air-ice CO_2 fluxes in the Arctic coastal zone (Amundsen Gulf, Beaufort Sea). *J. Geophys. Res.* **117**, C00G10, doi:10.1029/2011JC007118.

Geilfus N. X., Delille B., Verbeke V. and Tison J.-L. (2012b) Towards a method for high vertical resolution measurements of the partial pressure of CO_2 within bulk sea ice. *J. Glaciol.* **58**, 208-212.

Gleitz M., v.d. Loeff M. R., Thomas D. N., Dieckmann G. S. and Millero F. J. (1995) Comparison of summer and winter inorganic carbon, oxygen and nutrient concentrations in Antarctic sea ice brine. *Mar. Chem.* **51**, 81-91.

Golden K. M., Ackley S. F. and Lytle V. I. (1998) The percolation phase transition in sea ice. *Science* **282**, 2238-2241.

Goyet C. and Poisson A. (1989) New determination of carbonic acid dissociation constants in seawater as a function of temperature and salinity. *Deep-Sea Res.* **36**, 1635-1654.

Hales B., Chipman D. and Takahashi T. (2004a) High-frequency measurements of partial pressure and total concentration of carbon dioxide in seawater using microporous hydrophobic membrane contactors. *Limnol. Oceanogr. Methods* **2**, 356-364.

Hales B., van Greer A. and Takahashi T. (2004b) High-frequency measurements of seawater chemistry: Flow-injection analysis of macronutrients. *Limnol. Oceanogr. Methods* **2**, 91-101.

Hain M. P., Sigman D. M., Higgins J. A. and Haug G. H. (2015) The effects of secular calcium and magnesium concentration changes on the thermodynamics of seawater acid/base chemistry: Implications for Eocene and Cretaceous ocean carbon chemistry and buffering. *Global Biogeochem. Cycles* **29**, 517-533.

Hansson I. (1973) A new set of acidity constants for carbonic acid and boric acid in seawater. *Deep-Sea Res.* **20**, 461-478.

He S. and Morse J. W. (1993) The carbonic acid system and calcite solubility in aqueous Na-K-Ca-Mg-Cl-SO_4 solutions from 0 to 90°C. *Geochim. Cosmochim. Acta* **57**, 3533-3554.

Howarth R. W. (1978) A rapid and precise method for determining sulfate in seawater, estuarine waters, and sediment pore waters. *Limnol. Oceanogr.* **23**, 1066-1069.

Kennedy H., Thomas D. N., Kattner G., Haas C. and Dieckmann G. S. (2002) Particulate organic matter in Antarctic summer sea ice: concentration and stable isotopic composition. *Mar. Ecol. Prog. Ser.* **238**, 1-13.

Lee K., Kim T.-W., Byrne R. H., Millero F. J., Feely R. A. and Liu Y.-M. (2010) The universal ratio of boron to chlorinity for the North Pacific and North Atlantic oceans. *Geochim. Cosmochim. Acta* 74, 1801-1811.

Liu X., Patsavas M. C. and Byrne R. H. (2011) Purification and characterization of meta-Cresol Purple for spectrophotometric seawater pH measurements. *Environ. Sci. Technol.* 45, 4862-4868.

Loucaides S., Rérolle V. M. C., Papadimitriou S., Kennedy H., Mowlem M. C., Dickson A. G., Gledhill M. and Achterberg E. P. (2017) Characterization of *meta*-Cresol Purple for spectrophotometric pH measurements in saline and hypersaline media at sub-zero temperatures. *Sci. Rep.* **7**, 2481, doi:10.1038/s41598-017-02624-0

Lueker T. J., Dickson A. G. and Keeling C. D. (2000) Ocean pCO_2 calculated from dissolved inorganic carbon, alkalinity, and equations for K_1 and K_2: validation based on laboratory measurements of CO_2 in gas and seawater at equilibrium. *Mar. Chem.* 70, 105-119.

Marion G. M. (2001) Carbonate mineral solubility at low temperatures in the Na-K-Mg-Ca-H-Cl-SO_4-OH-HCO_3-CO_3-CO_2-H_2O system. *Geochim. Cosmochim. Acta* **65**, 1883–1896.

Marion G. M., Mironenko M. V. and Roberts M. W. (2010) FREZCHEM: A geochemical model for cold aqueous solutions. *Comput. Geosci.* **36**, 10-15.

Mehrbach C., Culberson C. H., Hawley J. E. and Pytkowicz R. M. (1973) Measurement of the apparent dissociation constants of carbonic acid in seawater at atmospheric pressure. *Limnol. Oceanogr.* **18**, 897-907.

Miller L. A., Fripiat F., Else B. G. T., Bowman J. S., Brown K. A., Collins R. E., Ewert M., Fransson A., Gosselin M., Lannuzel D., Meiners K. M., Michel C., Nishioka J., Nomura D., Papadimitriou S., Russell L. M., Sørensen L. L., Thomas D. N., Tison J.-L., van Leeuwe M. A., Vancoppenolle M., Wolff E.W., Zhou J. (2015) Methods for biogeochemical studies of sea ice: The state of the art, caveats, and recommendations. *Elementa: Science of the Anthropocene* **3**, 000038, doi: 10.12952/journal.elementa.000038.

Miller L. A., Carnat G., Else B. G. T., Sutherland N. and Papakyriakou T. N. (2011a) Carbonate system evolution at the Arctic Ocean surface during autumn freeze-up. *J. Geophys. Res.* **116**, C00G04, doi: 10.1029/2011JC007143.

Miller L. A., Papakyriakou T. N., Collins R. E., Deming J. W., Ehn J. K., Macdonald R. W., Mucci A., Owens O., Raudsepp M. and Sutherland N. (2011b) Carbon dynamics in sea ice: A winter flux time series. *J. Geophys. Res.* **116**, C02028, doi: 10.1029/2009JC006058.

Millero F. J. (1995) Thermodynamics of the carbon dioxide system in the oceans. *Geochim. Cosmochim. Acta* **59**, 661–677.

Millero F. J. and Huang F. (2009) The density of seawater as a function of salinity (5 to 70 g kg^{-1}) and temperature (273.15 to 363.15 K). *Ocean Sci.* **5**, 91-100.

Millero, F.J., Zhang, J.Z., Fiol, S., Sotolongo, S., Roy, R.N., Lee K., Mane S. (1993) The use of buffers to measure the pH of seawater. *Mar. Chem.* **44**, 143-152.

Millero F. J., Pierrot D., Lee K., Wanninkhof R., Feely R., Sabine C. L., Key R. M. and Takahashi T. (2002) Dissociation constants for carbonic acid determined from field measurements. *Deep-Sea Res. Part I* **49**, 1705-1723.

Millero F. J., Graham T. B., Huang F., Bustos-Serrano H. and Pierrot D. (2006) Dissociation constants of carbonic acid in seawater as a function of salinity and temperature. *Mar. Chem.* **100**, 80-94.

Millero F. J., Feistel R., Wright D. G. and McDougall T. J. (2008) The composition of standard seawater and the definition of the reference-composition salinity. *Deep-Sea Res Part I* **55**, 50-72.

Mohica-Prieto F. J. and Millero F. J. (2002) The values of $pK_1 + pK_2$ for the dissociation of carbonic acid in seawater. *Geochim. Cosmochim. Acta* **66**, 2529–2540.

Munro D. R., Dunbar R. B., Mucciarone D. A., Arrigo K. R. and Long M. C. (2010) Stable isotopic composition of dissolved inorganic carbon and particulate organic carbon in sea ice from the Ross Sea, Antarctica. *J. Geophys. Res.* **115**, C09005, doi:10.1029/2009JC005661.

Papadimitriou S., Kennedy H., Kattner G., Dieckmann G. S. and Thomas D. N. (2004) Experimental evidence for carbonate precipitation and CO_2 degassing during sea ice formation. *Geochim. Cosmochim. Acta* **68**, 1749-1761.

Papadimitriou S., Thomas D. N., Kennedy H., Haas C., Kuosa H., Krell H. and Dieckmann D. S. (2007) Biogeochemical composition of natural sea ice brines from the Weddell Sea during early austral summer. *Limnol. Oceanogr.* **52**, 1809-1823.

Papadimitriou S., Kennedy H., Norman L., Kennedy D. P. and Thomas D. N. (2012) The effect of biological activity, $CaCO_3$ mineral dynamics, and CO_2 degassing in the inorganic carbon cycle in sea ice in late winter-early spring in the Weddell Sea, Antarctica. *J. Geophys. Res.* **117**, C08011, doi: 10.1029/2012JC008058.

Papadimitriou S., Kennedy H., Kennedy P. and Thomas D. N. (2013) Ikaite solubility in seawater-derived brines at 1 atm and sub-zero temperatures to 265 K. *Geochim. Cosmochim. Acta* **109**, 241-253, doi:10.1016/j.gca.2013.01.044.

Papadimitriou S., Kennedy H., Kennedy P. and Thomas D. N. (2014) Kinetics of ikaite precipitation and dissolution in seawater-derived brines at subzero temperatures to 265 K. *Geochim. Cosmochim. Acta* **140**, 199-211, doi: 10.1016/j.gca.2014.05.031.

Papadimitriou S., Loucaides S., Rérolle V. M. C., Achterberg E. P., Dickson A. G., Mowlem M. C. and Kennedy H. (2016) The measurement of pH in saline and hypersaline media at sub-zero temperatures: Characterization of Tris buffers. *Mar. Chem.***184**, 11-20.

Pierrot D., Neill C., Sullivan K., Castle R., Wanninkhof R., Lüge H., Johannessen T., Olsen A., Feely R. A. and Cosca C. E. (2009) Recommendations for autonomous underway pCO_2 measuring systems and data reduction techniques. *Deep-Sea Res Part II* **56**, 512-522.

Pitzer K. S. (1973) Thermodynamics of electrolytes. I. Theoretical basis and general equations. *J. Phys. Chem.* **77**, 268–277.

Plummer N. L. and Busenberg E. (1982) The solubility of calcite, aragonite, and vaterite in CO_2-water solutions between 0 – 90 °C and an evaluation of the aqueous model for the system CO_2-H_2O-$CaCO_3$. *Geochim. Cosmochim. Acta* **46**, 1011-1040.

Pytkowicz R. M. and Kester D. R. (1969) Harned's rule behaviour of NaCl–Na_2SO_4 solutions explained by an ion association model. *Am. J. Sci.* **267**, 217–229.

Rérolle V. M. C., Floquet C. F. A., Harris A. J. K., Mowlem M. C., Bellerby R. R. G. J. and Achterberg E. P. (2013) Development of a colorimetric microfluidic pH sensor for autonomous seawater measurements. *Anal. Chim. Acta* **786**, 124-131.

Roy R. N., Roy L. N., Lawson M., Vogel K. M., Porter-Moore C., Davis W., Millero F. J. and Campbell D. M. (1993) The dissociation constants of carbonic acid in seawater at salinities 5 to 45 and temperatures 0 to 45 °C. *Mar. Chem.* **44**, 249-259.

Rysgaard S., Glud R. N., Sejr M. K., Bendtsen J. and Christensen P. B. (2007) Inorganic carbon transport during sea ice growth and decay: A carbon pump in polar seas. *J. Geophys. Res. Oceans* **112**, C03016, doi: 10.1029/2006JC003572.

Rysgaard S., Bendtsen J., Delille B., Dieckmann G. S., Glud R. N., Kennedy H., Mortensen J., Papadimitriou S., Thomas D. N. and Tison J.-L. (2011) Sea ice contribution to the air–sea CO_2 exchange in the Arctic and Southern Oceans. *Tellus B* **63**, 823-830.

Sabine C. L., Feely R. A., Gruber N., Key R. M., Lee K., Bullister J. L., Wanninkhof R., Wong C. S., Wallace D. W. R., Tilbrook B., Millero F. J., Peng T.-H., Kozyr A., Ono T., Rios A. F. (2004) The oceanic sink for anthropogenic CO_2. *Science* **305**, 367-371.

Semiletov I., Pipko I., Gustafsson Ö., Anderson L. G., Sergienko V., Pugach S., Dudarev O., Charkin A., Gukov A., Bröder L., Andersson A., Spivak E. and Shakhova N. (2016) Acidification of East Siberian Arctic Shelf waters through addition of freshwater and terrestrial carbon. *Nat. Geosci.* **9**, 361-365.

Takahashi T. (2004) The fate of industrial carbon dioxide. *Science* **305**, 352-353.

Takahashi T., Sutherland S. C., Chipman D. W., Goddard J. G., Ho C., Newberger T., Sweeney C. and Munro D. R. (2014) Climatological distributions of pH, pCO_2, total CO_2, alkalinity, and $CaCO_3$ saturation in the global surface ocean, and temporal changes at selected locations. *Mar. Chem.* **164**, 95-125.

Takahashi T., Feely R. A., Weiss R. F., Wanninkhof R. H., Chipman D. W., Sutherland S. C. and Takahashi T. T. (1997) Global air-sea flux of CO_2: An estimate based on measurements of sea-air pCO_2 difference. *Proc. Natl.Acad. Sci. USA* **94**, 8292-8299.

Thomas D. N. and Dieckmann G. S. (2002) Sea ice – A habitat for extremophiles. *Science* **295**, 641-644.

Turner D. R., Achterberg E. P., Chen C.-T. A., Clegg S. L., Hatje V., Maldonado M., Sander S. G., van den Berg C. M. G. and Wells M. (2016) Toward a quality-controlled and accessible Pitzer model for seawater and related systems. *Front. Mar. Sci.* **3**, 139, doi:10.3389/fmars.2016.00139.

UNESCO (1983). Algorithms for computation of fundamental properties of seawater. UNESCO Technical Papers in Marine Science 44, 53 pp.

Weiss R. S. (1974) Carbon dioxide in water and seawater: The solubility of a non-ideal gas. *Mar. Chem.* **2**, 203-215.

Yamamoto-Kawai M., McLaughlin F. A., Carmack E. C., Nishino S. and Shimada K. (2009) Aragonite undersaturation in the Arctic Ocean: Effects of ocean acidification and sea ice melt. *Science* **326**, 1098-1100.

List of Figures

Figure 1. The stoichiometric equilibrium first and second dissociation constants of carbonic acid as negative common logarithm versus temperature (open circles) in natural seawater (S_P = 33 – 34). The curves were derived from the salinity-temperature functions in Lueker et al. (2000) based on the measurements of Mehrbach et al. (1973) (dashed line) and from the measurements on the seawater proton scale of Millero et al. (2006), converted to the total proton scale as in Millero (1995) and re-fitted here (solid line). Note the difference in the scale of the *y*-axis in the pK^*_{1C} and pK^*_{2C} panels.

Figure 2. The stoichiometric equilibrium first and second dissociation constants of carbonic acid as negative common logarithm versus salinity from this study (open circles) and from Millero et al. (2006) (crosses) when available at 20 °C [panels (a) and (b)], 5 °C [panels (c) and (d)], 0 °C [panels (e) and (f)], and the freezing point [panels (g) and (h)]. The dashed curve represents the salinity-temperature functions in Lueker et al. (2000) based on the measurements of Mehrbach et al. (1973), extrapolated outside their empirical range of S_P = 19 – 43 and for t < 2.0 °C. The solid curve represents the salinity-temperature functions based on the measurements on the seawater proton scale of Millero et al. (2006), converted to the total proton scale and re-fitted here, and extrapolated outside their empirical range for S_P > 51 and for t < 1.0 °C. Note the difference in the scale of the *y*-axis in the pK^*_{1C} and pK^*_{2C} panels.

Figure 3. The stoichiometric equilibrium first and second dissociation constants of carbonic acid as negative common logarithm versus temperature in panels (a) and (b), and versus salinity in panels (c) and (d), respectively, at the freezing point of seawater and seawater-derived brine from this study (open circles) and from the output of the thermodynamic code FREZCHEM v15.1 (dashed line). Note the equivalent scale of the *y*-axis in the pK^*_{1C} and pK^*_{2C} panels.

Figure 4. Difference between observed and fitted values of the stoichiometric equilibrium first and second dissociation constants of carbonic acid as negative common logarithm in seawater and brines as a function of salinity [panels (a) and (b)] and temperature [panels (c) and (d)].

Figure 5. Change in pH in the total proton scale [panels (a), (d)], CO_2 fugacity [panels (b), (e)], and the total concentration of the carbonate ion [panels (c), (f)] in sea ice brine inclusions at ice-brine equilibrium (freezing point) as a function temperature in conservative seawater-derived brines with respect to major ionic composition, A_T, and C_T (upper panels), and in conservative brines at equilibrium with current atmospheric CO_2 (non-conservative C_T) (lower panels). The

values of the illustrated parameters were determined for equilibrium freezing of surface seawater from the western Weddell Sea, Antarctica, in Papadimitriou et al. (2012) by solving the system of equations that describe the chemical equilibria of the marine CO_2 system using the dissociation constants of carbonic acid from this study (solid line), and as computed from the salinity-temperature functions fitted to the measurements of Mehrbach et al. (1973) by Lueker et al. (2000) (dashed line) and to the measurements of Millero et al. (2006) following conversion to the total proton scale and re-fitting in this study (dotted line). Further details are given in *Section 2.7*.

Figure 6. The differences between the current data set and each of the two sets of extrapolated oceanographic pK^*_{1C} and pK^*_{2C} equations (Lueker et al., 2000; Millero et al., 2006) in respect of fCO_2 [ΔfCO_2: panels (a) and (b)] and pH on the total proton scale [ΔpH_T: panels (c) and (d)] computed from A_T and C_T at the freezing point as a function of the C_T to A_T ratio (C_T/A_T) of the brine system. The ΔfCO_2 and ΔpH_T are shown for S_P = 50 (squares), 60 (diamonds), 85 (circles), and 100 (triangles, crosses) for (*i*) the conservative brine A_T and C_T scenario (closed symbols; also illustrated in Fig. 5a, b), (*ii*) between measured pH_T and fCO_2 near the freezing point of experimental brines and their values derived from the relevant A_T and C_T measurements (Table 2) as computed using each of the two sets of extrapolated oceanographic pK^*_{1C} and pK^*_{2C} equations (open symbols), and (*iii*) for illustration purposes, for C_T/A_T decreasing from the conservative C_T/A_T scenario to lower values (conservative A_T, non-conservative C_T) at a constant t_{FP} = –6.0 °C and S_P = 100 (crosses).

Table 1. Major ion composition of brines (in mmol kg^{-1}).

Salinity	$[Na^+]$	$[Mg^{2+}]$	$[Ca^{2+}]$	$[K^+]$	$[Cl^-]+[Br^-]$	$[SO_4^{2-}]$
100.52	1347	150.64	29.96	25.85	1566	77.21
98.69	1323	148.89	28.99	26.26	1554	77.47
84.62	1134	128.02	25.00	22.26	1327	66.97
61.54	825	92.66	18.18	16.23	968	50.48
60.30	808	91.34	17.87	15.40	946	47.25
60.28	808	91.25	17.84	16.11	944	47.93
50.24	681	74.20	14.54	13.57	795	39.79
50.15		75.15	14.55			40.37
48.90		72.65	14.30			38.80
40.20	539	60.84	11.83	11.09	632	32.77
[a]35	470±2	52.60±0.45	10.29±0.10	9.27±0.23	550±2	27.82±0.54
[b]35	469	52.82	10.28	10.21	547	28.24

[a]mean concentration of brines normalized to salinity 35

[b]composition of Reference Seawater of salinity 35 (Millero et al., 2008)

Table 2. Practical salinity (S_P), temperature (*t*, in °C), phosphate (SRP) and silicic acid [$Si(OH)_4$] (in μmol kg^{-1}), the measured parameters of the carbonate system in seawater and seawater-derived brines [C_T (in μmol kg^{-1}), A_T and derived carbonate alkalinity (A_C) (in μmol kg^{-1}), fCO_2 (in μatm), and pH_T (total proton scale; in mol kg^{-1})], and the stoichiometric equilibrium first and second dissociation constants of carbonic acid (in mol kg^{-1}, total proton scale) as negative common logarithms (pK^*_{1C} and pK^*_{2C}).

S_P	SRP	$Si(OH)_4$	*t*	C_T	A_T	A_C	fCO_2	pH_T	pK^*_{1C}	pK^*_{2C}
33.14	0.1	2.9	–1.79	2047	2259	2177	184	8.345	6.167	9.468
33.54	0.0	8.1	17.98	2042	2282	2200	369	8.052	5.889	9.089
33.64	0.3	3.8	–1.53	2153	2287	2231	329	8.125	6.163	9.432
			–1.53	2157	2287	2231	329	8.122	6.158	9.448
			–1.53	2154	2287	2232	331	8.118	6.158	9.425
			22.01	2139	2287	2233	788	7.780	5.866	9.007
33.64	0.3	3.8	15.07	2114	2281	2221	520	7.934	5.932	9.126
			15.07	–	2281	2221	519	7.929	–	–
			15.11	2119	2281	2220	518	7.935	5.928	9.151
			25.01	2144	2281	2229	887	7.731	5.832	8.991
			25.02	2138	2281	2228	872	7.737	5.833	8.977
			25.06	2141	2281	2228	880	7.732	5.830	8.984
33.94	0.0	7.1	–1.17	2063	2278	2194	186	8.333	6.143	9.457
			–1.06	2073	2278	2199	206	8.298	6.148	9.436
			–1.06	–	2278	2199	203	8.298	–	–
			–0.03	2045	2278	2192	186	8.329	6.127	9.401
			0.04	2064	2278	2194	201	8.309	6.132	9.435
			0.04	2061	2278	2195	202	8.308	6.135	9.420
			0.04	2061	2278	2195	201	8.305	6.130	9.418
			5.03	2050	2278	2195	237	8.232	6.052	9.309
			9.94	2048	2278	2198	280	8.148	5.968	9.210
			20.04	2044	2278	2202	433	7.986	5.866	9.019
			24.96	2100	2278	2213	676	7.835	5.831	9.003
			24.99	2100	2278	2214	682	7.832	5.832	8.996
			25.04	2091	2278	2213	680	7.833	5.835	8.968
34.04	0.2	4.8	0.00	2053	2286	2199	191	8.327	6.134	9.403
			0.00	2054	2286	2199	190	8.324	6.128	9.403
			0.00	–	2286	2199	191	8.323	–	–
			0.06	2049	2286	2195	181	8.350	6.133	9.427
			20.03	2050	2286	2206	430	8.005	5.880	9.045
			20.03	2048	2286	2206	420	8.004	5.870	9.039
			20.03	2048	2286	2206	427	8.004	5.877	9.039

Table 2 (continued)

S_P	SRP	$Si(OH)_4$	t	C_T	A_T	A_C	fCO_2	pH_T	pK^*_{1C}	pK^*_{2C}
40.20	0.1	46.9	–2.15	2512	2806	2703	216	8.327	6.123	9.375
			4.97	2584	2806	2729	426	8.071	6.025	9.229
48.90	0.0	259.4	–2.72	3177	3528	3411	347	8.247	6.134	9.300
			-0.09	3155	3528	3413	385	8.198	6.092	9.206
			20.05	3142	3528	3420	851	7.883	5.841	8.850
50.15	0.0	55.2	–2.74	3026	3481	3329	224	8.397	6.123	9.326
			–2.74	3038	3481	3337	248	8.366	6.134	9.300
50.24	0.0	38.3	–1.56	2947	3446	3296	232	8.373	6.114	9.223
			–0.06	2976	3446	3306	268	8.312	6.082	9.191
			4.88	2976	3446	3308	329	8.233	6.013	9.109
			10.00	2944	3446	3306	383	8.168	5.949	8.998
			15.00	2984	3446	3318	532	8.051	5.896	8.921
			25.05	2977	3446	3323	807	7.895	5.807	8.743
60.28	0.4	15.3	–3.36	3645	4116	3965	379	8.284	6.137	9.264
			–0.27	3643	4116	3968	419	8.229	6.073	9.202
			25.02	3627	4116	3987	1183	7.802	5.765	8.718
60.30	1.2	26.9	–3.37	3641	4180	4012	302	8.340	6.101	9.259
			–2.40	3652	4180	4016	308	8.310	6.060	9.240
			–2.37	3661	4180	4016	318	8.308	6.069	9.250
			20.29	3649	4180	4035	864	7.925	5.802	8.819
61.54	0.4	0.5	–3.46	3707	4228	4060	328	8.331	6.115	9.279
			–0.11	3705	4228	4062	370	8.276	6.056	9.219
84.62	1.0	18.0	–4.97	4863	5811	5562	371	8.409	6.118	9.167
			–4.93	4842	5811	5560	366	8.413	6.120	9.155
			0.04	4840	5811	5567	455	8.318	6.035	9.054
			5.02	4855	5811	5579	583	8.216	5.960	8.954
			20.33	4847	5811	5599	1088	7.953	5.773	8.668
98.69	1.4	22.6	–6.00	5457	6795	6486	392	8.509	6.196	9.130
			–5.93	5454	6795	6483	356	8.512	6.156	9.134
			0.03	5459	6795	6498	459	8.390	6.042	9.007
			4.87	5441	6795	6504	546	8.304	5.960	8.907
100.52	2.0	20.7	–5.98	5628	6901	6611	417	8.469	6.157	9.129
			20.30	5656	6901	6673	1308	7.946	5.755	8.587

Table 3. Best fit values for the coefficients of the salinity-temperature functions of the first and second stoichiometric equilibrium dissociation constants of carbonic acid in seawater and seawater-derived brines on the total proton scale.

		data set			
		Millero et al. (2006)		this study	
Parameter	Coefficient	pK^*_{1C}	pK^*_{2C}	pK^*_{1C}	pK^*_{2C}
$S_P^{0.5}$	a_o	13.47667	21.07076	6.14528	27.557655
S_P	a_1	0.032404	0.12322	–0.127714	0.154922
S_P^2	a_2	$–5.534\times10^{–5}$	$–3.68\times10^{–4}$	$7.396\times10^{–5}$	$–2.48396\times10^{–4}$
$S_P^{0.5}$ /T	a_3	–535.036	–774.97	–622.886	–1014.819
S_P/T	a_4	–5.8655	–19.5835	29.714	–14.35223
$S_P^{0.5}$ lnT	a_5	–2.07643	–3.328487	–0.666812	–4.4630415
constant	b_o	[a] –126.34048	[a] –90.18333	–176.48	–323.52692
1/T	b_1	[a] 6320.813	[a] 5143.692	9914.37	14763.287
lnT	b_2	[a] 19.568224	[a] 14.613358	26.05129	50.385807
user confirmation value S_P = 35, T = 273.15 K		6.1184	9.3827	6.1267	9.3940

[a] from Millero et al. (2006)

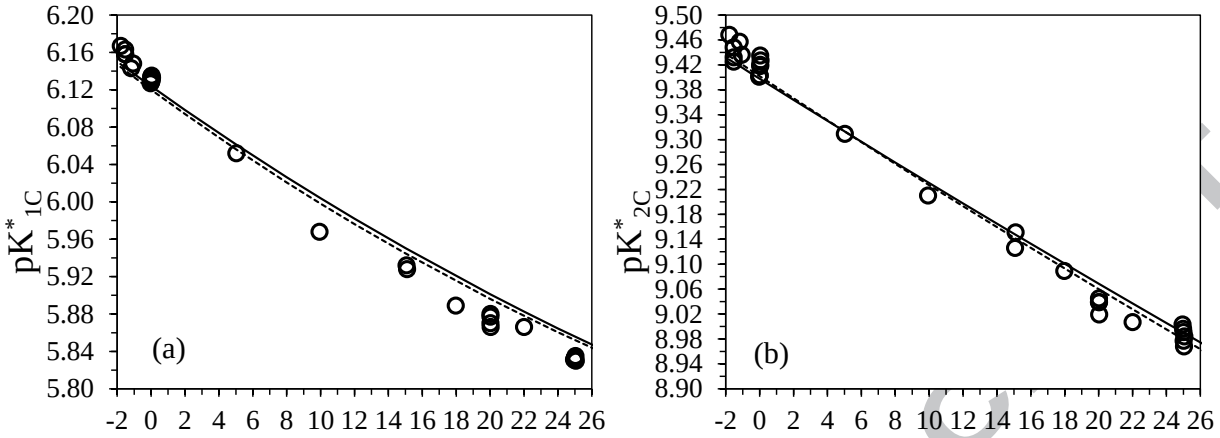

Figure 1
Papadimitriou et al.

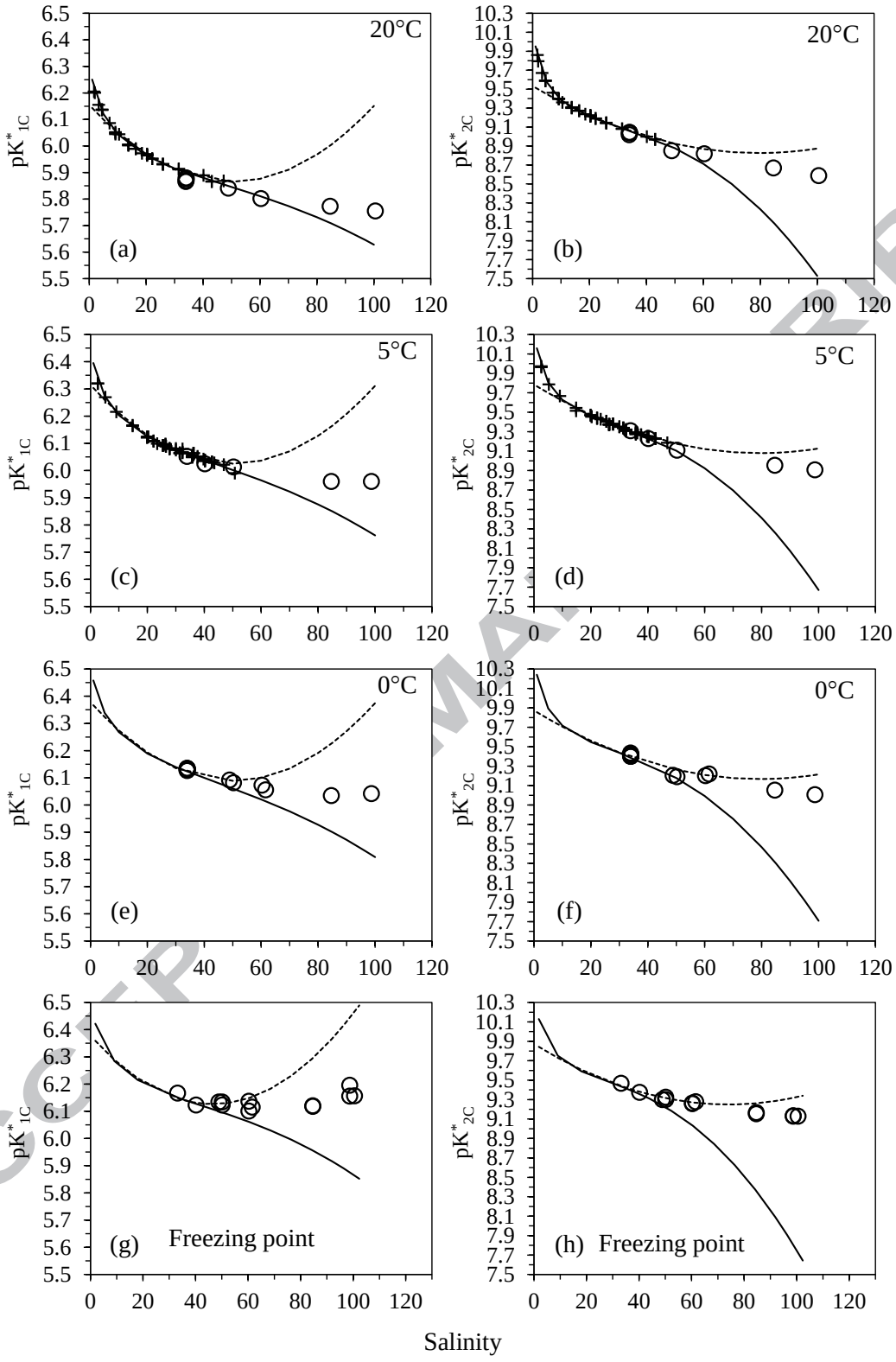

Figure 2
Papadimitriou et al.

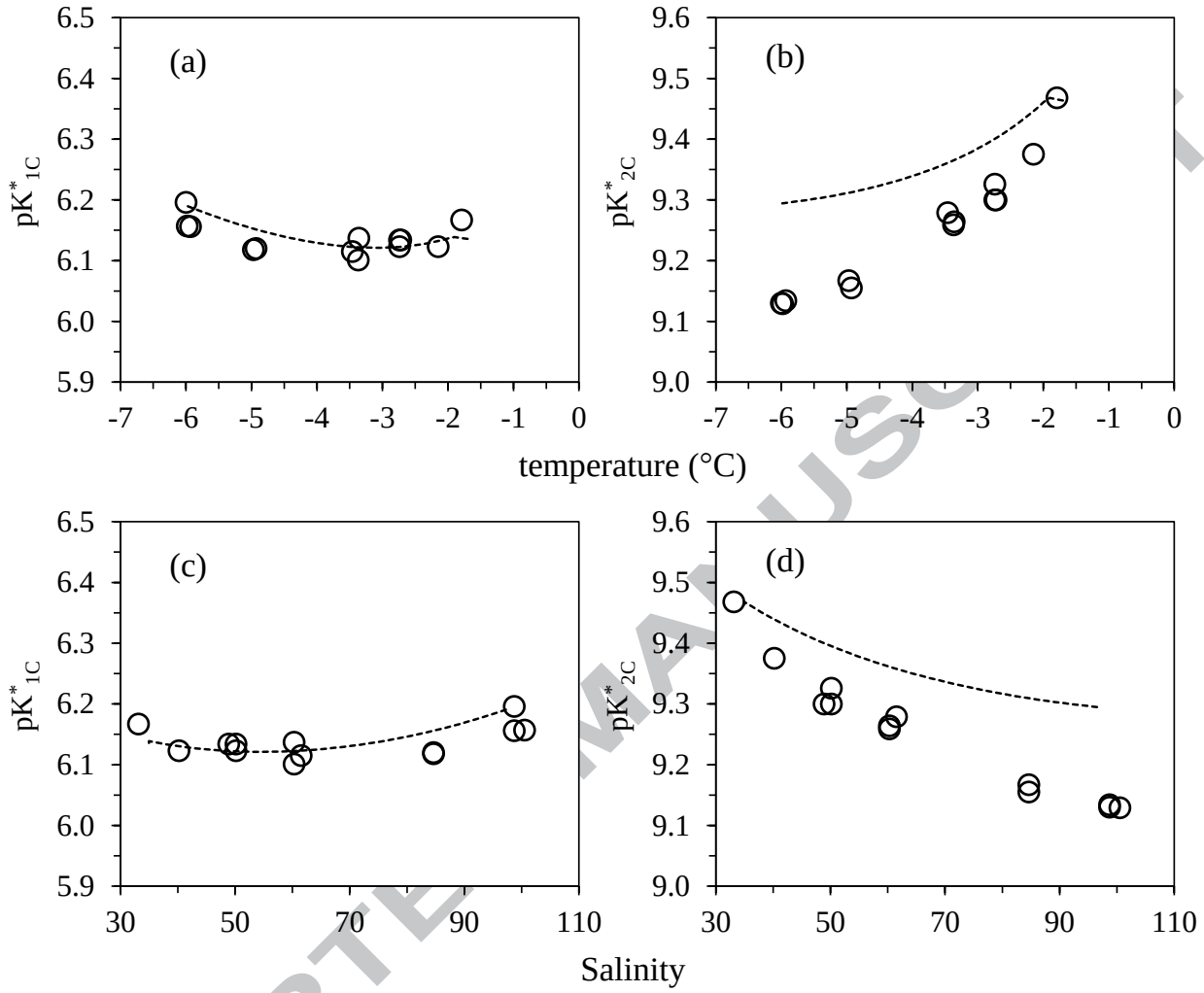

Figure 3
Papadimitriou et al.

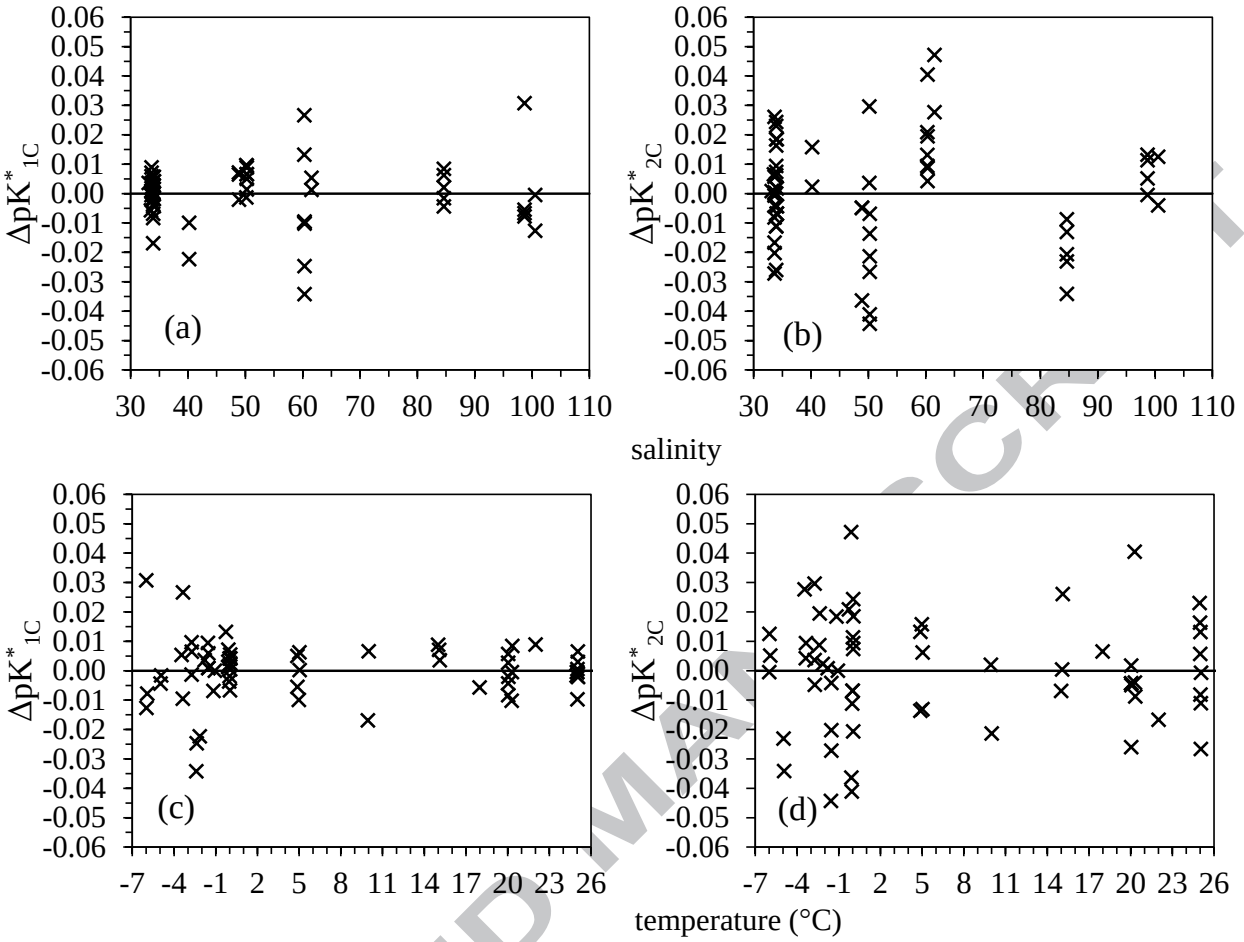

Figure 4
Papadimitriou et al.

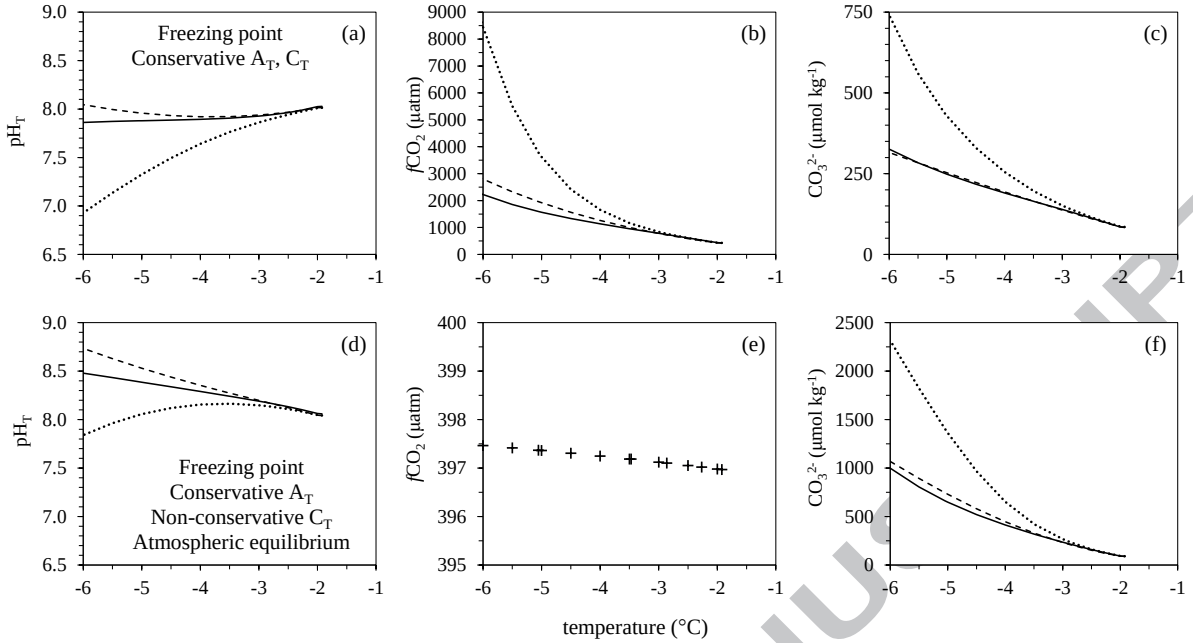

Figure 5
Papadimitriou et al.

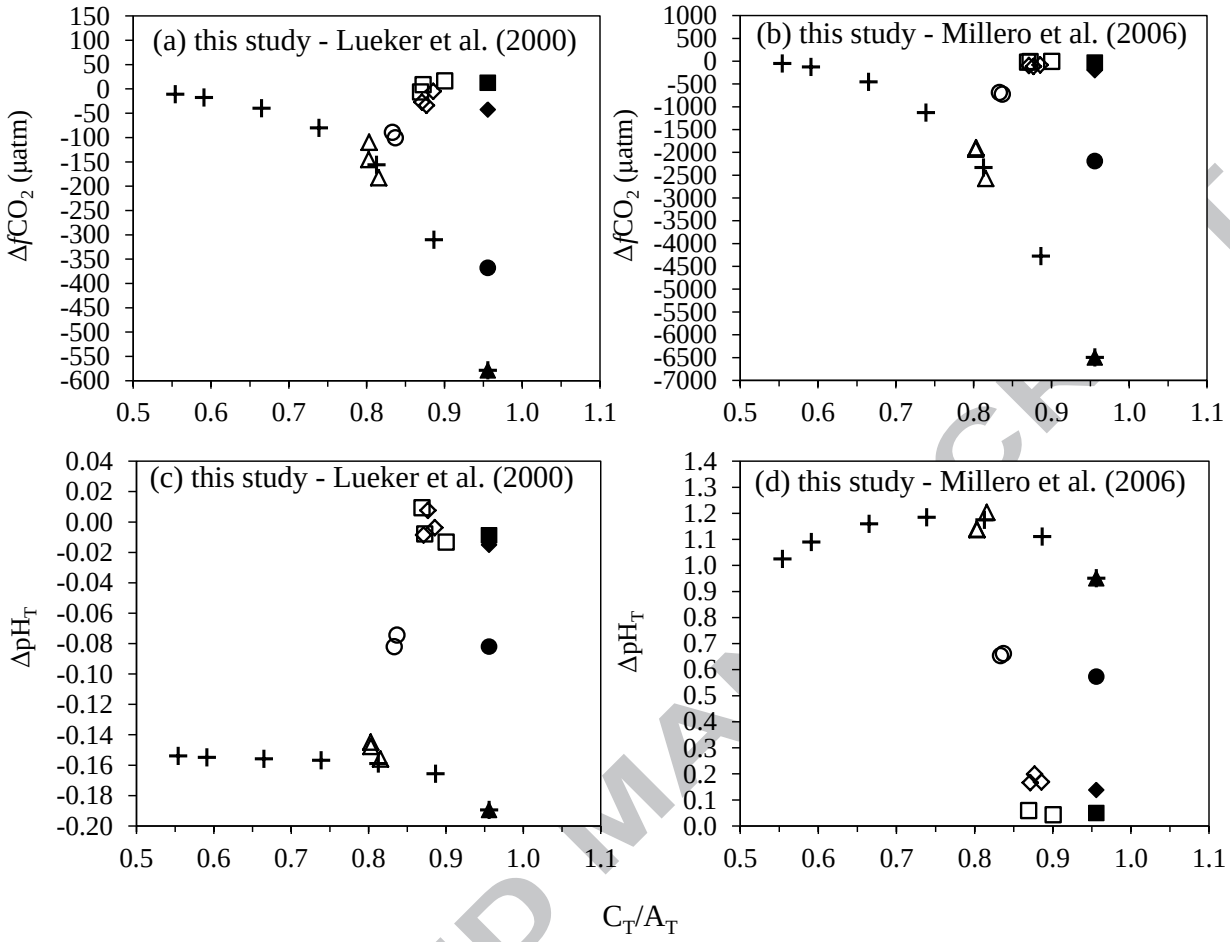

Figure 6
Papadimitriou et al.